Tonic inhibition mediates a synchronisation enhancement during propofol anaesthesia in a network of hippocampal interneurons: a modelling study

Laure Buhry, Francesco Giovannini

Tonic inhibition mediates a synchronisation enhancement during propofol anaesthesia in a network of hippocampal interneurons: a modelling study

Laure Buhry , Francesco Giovannini

Tonic inhibition mediates a synchronisation enhancement during propofol anaesthesia in a network of hippocampal interneurons: a modelling study

Laure Buhry *, Francesco Giovannini *

Project-Team Neurosys

Abstract: Neural oscillations are thought to be correlated with the execution of cognitive functions. Indeed, gamma oscillations are often recorded in functionally-coupled brain regions for cooperation during memory tasks, and this rhythmic behaviour is thought to result from synaptic GABAergic interactions between interneurons. Interestingly, GABAergic synaptic and extrasynaptic receptors have been shown to be the preferred target of the most commonly used anaesthetic agents. We present a in-depth computational study of the action of anaesthesia on neural oscillations by introducing a new mathematical model which takes into account the four main effects of the anaesthetic agent propofol on GABAergic hippocampal interneurons. These are: the action on synaptic $GABA_A$ receptors, which includes an amplification and an extension of the duration of the synaptic currents, as well as an increase in current baseline, and the action on extrasynaptic $GABA_A$ receptors mediating a tonic inhibitory current. Our results indicate that propofol-mediated tonic inhibition contributes to an unexpected enhancement of synchronisation in the activity of a network of hippocampal interneurons. We speculate that this enhanced synchronisation could provide a possible mechanism supporting the occurrence of intraoperative awareness and explicit memory formationunder general anaesthesia, by transiently facilitating the communication between brain structures which should supposedly be not allowed to do so when anaesthetised.

Key-words: general anesthesia, computational modeling, propofol, Hodgkin-Huxley model, extrasynaptic inhibition

* LORIA UMR 7503, Université de Lorraine, Vandoeuvre-lès-Nancy, F-54500, France, Tel.: +33 (0)3 8359 3092, Fax: +33 (0)3 8359 3000, Email: laure.buhry@loria.fr

Tonic inhibition mediates a synchronisation enhancement during propofol an aesthesia in a network of hippocampal interneurons: a modelling study

Résumé : Neural oscillations are thought to be correlated with the execution of cognitive functions. Indeed, gamma oscillations are often recorded in functionally-coupled brain regions for cooperation during memory tasks, and this rhythmic behaviour is thought to result from synaptic GABAergic interactions between interneurons. Interestingly, GABAergic synaptic and extrasynaptic receptors have been shown to be the preferred target of the most commonly used anaesthetic agents. We present a in-depth computational study of the action of anaesthesia on neural oscillations by introducing a new mathematical model which takes into account the four main effects of the anaesthetic agent propofol on GABAergic hippocampal interneurons. These are: the action on synaptic $GABA_A$ receptors, which includes an amplification and an extension of the duration of the synaptic currents, as well as an increase in current baseline, and the action on extrasynaptic $GABA_A$ receptors mediating a tonic inhibitory current. Our results indicate that propofol-mediated tonic inhibition contributes to an unexpected enhancement of synchronisation in the activity of a network of hippocampal interneurons. We speculate that this enhanced synchronisation could provide a possible mechanism supporting the occurrence of intraoperative awareness and explicit memory formationunder general anaesthesia, by transiently facilitating the communication between brain structures which should supposedly be not allowed to do so when anaesthetised.

Mots-clés : general anesthesia, computational modeling, propofol, Hodgkin-Huxley model, extrasynaptic inhibition

1 Introduction

General anaesthesia is a reversible drug-induced coma which is commonly administered to patients undergoing surgery due to its desirable properties, which are: loss of consciousness, analgesia, immobility, and amnesia, all obtained whilst preserving physiological stability [Brown et al., 2010]. Indeed, after the induction of general anaesthesia, patients enter a state of sedation during which they are not aware of the surgery, they do not perceive nor react to the noxious stimuli deriving from it, and they do not remember undergoing it. These properties derive from the combined action of an hypnotic agent, an analgesic (to avoid pain), and a curariform skeletal muscle relaxant or neuromuscular blocker (to induce immobility). Although having become a standard operating procedure during surgery – in the United States alone, approximately 60000 patients undergo general anaesthesia every day [Brown et al., 2010] – the chemical and neuronal mechanisms by which these effects are obtained are yet to be fully unravelled.

Loss of consciousness is achieved by the injection or gas inhalation of an hypnotic agent like the widely used propofol. Propofol, 2,6-di-isopropyl-phenol, [Vanlersberghe and Camu, 2008] is one of the main anaesthetic intravenous agents used in surgical operations for the induction and maintenance of general anaesthesia. Propofol-induced sedation is obtained by globally potentiating GABAergic inhibitory activity [Adodra and Hales, 1995, Bai et al., 1999, Bai et al., 2001, Kitamura et al., 2004, McDougall et al., 2008, Song et al., 2011], as the drug binds on $GABA_A$ receptors, both synaptic and extrasynaptic, enhancing their activation [Garcia et al., 2010, Nelson et al., 2002, Rudolph and Antkowiak, 2004, Zhou et al., 2012]. Four main molecular mechanisms are thought to underlie propofol-induced general anaesthesia:

1. An enhancement of the amplitude of $GABA_A$-mediated tonic currents by activating extrasynaptic $GABA_A$ receptors [Bai et al., 2001, McDougall et al., 2008, Song et al., 2011]

2. A potentiation of $GABA_A$-mediated synaptic currents by increasing the conductance of synaptic $GABA_A$ receptors [Adodra and Hales, 1995, McDougall et al., 2008]

3. An increase in the baseline of $GABA_A$-mediated synaptic currents by slowing the desensitisation of $GABA_A$ receptors [Bai et al., 1999, Bai et al., 2001, McDougall et al., 2008]

4. An extension in the duration of $GABA_A$-mediated synaptic currents by increasing the closing time of synaptic $GABA_A$ receptors [Bai et al., 2001, Kitamura et al., 2004, McDougall et al., 2008]

Here, we present a novel detailed model of anaesthetic action, including all four of the afore-mentioned effects, on neural oscillations mediated by GABAergic transmission. Synaptic GABAergic interactions between interconnected inhibitory neurons are thought to play an important role in the generation and maintenance of rhythmic neural activity, in particular in the γ-band $(20-80)\,Hz$ [Bartos et al., 2007, Cobb et al., 1995, Jonas et al., 2004]. Oscillations arise because inhibitory neurons provide their postsynaptic targets with precise windows of reduced excitability, and consequently of increased excitability once the inhibition fades away. We model a network of interconnected inhibitory interneurons whose activity tends to display, in the absence of propofol, loosely synchronous activity in the gamma range [Wang and Buzsáki, 1996]. Our results indicate that increasing the concentration of the anaesthetic agent yields a dosage-dependent enhancement of network synchronisation. This enhancement could facilitate the communication between brain structures [Fries, 2005] which, being anaesthetised, should supposedly be not allowed to do so. We hypothetise that this could provide a possible explanation for the emergence of unwanted behaviours under general anaesthesia, including intraoperative awareness and implicit memory formation.In addition, the transient characteristics of this phenomenon could explain the variability between different studies and patients.

2 Methods

We modelled the four afore-mentioned effects of propofol on a population of Hodgkin-Huxley hippocampal interneurons as follows.

2.1 Fast-Spiking Hippocampal Interneurons

We modelled fast-spiking hippocampal GABAergic interneurons using the Hodgkin-Huxley formalism, adapting the model described in [Kopell et al., 2010] and [Hutt and Buhry, 2014]. The current-balance equation takes the form:

$$C_m \cdot \frac{\mathrm{d}V_m}{\mathrm{d}t} = -I_l - I_K - I_{Na} - I_{syn} - I_{ton} \tag{1}$$

where I_l is the leak current, I_K is the potassium current, I_{Na} is the sodium current, I_{syn} is the inhibitory current deriving from synaptic GABAergic interactions, and I_{ton} is the tonic inhibitory current mediated by extrasynaptic GABA$_A$ receptors.

The transmembranal ionic currents are described by the following equations:

$$I_l = \overline{g}_l \cdot (V_m - E_l)$$

$$I_K = \overline{g}_K \cdot n^4 \cdot (V_m - E_K)$$

$$I_{Na} = \overline{g}_{Na} \cdot m^3 \cdot h \cdot (V_m - E_{Na})$$

where, m, h and n are activation variables which obey the following rules:

$$\frac{\mathrm{d}x}{\mathrm{d}t} = \frac{x_\infty - x}{\tau_x}$$
$$x_\infty = \frac{\alpha_x}{\alpha_x + \beta_x}$$
$$\tau_x = \frac{10}{7 \cdot (\alpha_x + \beta_x)}$$

for $x \in \{\, n, m, h \,\}$. The α and β functions for each activation variable are defined as:

$$\alpha_n = \frac{0.01 \cdot (V_m + 34)}{1 - \exp(-0.1 \cdot (V_m + 34))}$$

$$\beta_n = 0.125 \cdot \exp\left(-\frac{(V_m + 44)}{80}\right)$$

$$\alpha_m = \frac{0.1 \cdot (V_m + 35)}{1 - \exp\left(-\frac{(V_m + 35)}{10}\right)}$$

$$\beta_m = 4 \cdot \exp\left(-\frac{(V_m + 60)}{18}\right)$$

$$\alpha_h = 0.07 \cdot \exp\left(-\frac{(V_m + 58)}{20}\right)$$

$$\beta_h = \frac{1}{\exp(-0.1 \cdot (V_m + 28)) + 1}$$

2.2   Modelling the Effects of Anaesthetics on GABA$_A$ Receptors

2.2.1   Synaptic Phasic Inhibition

The equation for the synaptic takes the form:

$$I_{syn} = I_i = g_i \cdot (V_m - E_i) + k_{bas} \tag{2}$$

where g_i is the synaptic conductance which obeys the following rule, given its time decay constant τ_i:

$$\frac{\mathrm{d}g_i}{\mathrm{d}t} = -\frac{g_i}{\tau_i} \tag{3}$$

Whenever a postsynaptic neuron receives a presynaptic spike its conductance g_i is increased as follows: $g_i \leftarrow g_i + w_i$, where w_i is the connection weight between the interneurons. Propofol binds on synaptic $GABA_A$ receptors enhancing their conductance [Adodra and Hales, 1995] and increasing their closing time [Bai et al., 1999]. We modelled this effect by acting on the inhibitory synaptic weights w_i and decay time τ_i parameters as in [McCarthy et al., 2008]. Increasing propofol dosage reflects in an increase in both of these values.

In addition, we modelled the slowing desensitisation of $GABA_A$ receptors caused by exposure to propofol [Bai et al., 1999, Bai et al., 2001, McDougall et al., 2008] by appropriately modifying the baseline of the postsynaptic current k_{bas} etween 0 and 100 pA, the literature giving $0 \geq k_{bas} \leq 60$ ([McDougall et al., 2008]). The baseline is the synaptic current received by neurons when all their presynaptic afferents are quiescent. In the absence of propofol this parameter was set to $k_{bas} = 0\,pA$. Since the synaptic conductance g_i obeys the rule described in Equation 3, $k_{bas} = 0\,pA$ indicates that the synaptic current decays to $0\,pA$ as the ionic channel closes. However, increasing the value of k_{bas} ensures that the synaptic current does not dip below the specified baseline. To the best of our knowledge, propofol-induced receptor desensitisation has never been modelled in existing computational studies. Let us note that concentrations of propofol higher than $1\mu M$ are not physiological.

2.2.2   Extrasynaptic Tonic Inhibition

The action of propofol on extrasynaptic GABAergic receptors was modelled by varying the conductance g_{ton} of the tonic current I_{ton}, which takes the form:

$$I_{ton} = g_{ton} \cdot (V_m - E_i) \tag{4}$$

as described in [Hutt and Buhry, 2014], where E_i is the same reversal potential used for the synaptic inhibitory current I_i to maintain the equivalence between tonic and shunting inhibition. Increasing propofol dosage reflects in an increase in the tonic conductance g_{ton}, as described in the literature [McDougall et al., 2008, Song et al., 2011]. This produces a non-inactivating tonic inhibitory current which is not governed by activation-deactivation kinetics, as is the case for its synaptic counterpart. phenomenon is probably comparable to the synchrony observed in inhibitory networks where the decay time of the inhibition is very long [Rinzel and Ermentrout, 1998] since here, the inhibitory conductance is kept constant.

2.3   Network Configuration

Our network model comprised 100 fast-spiking hippocampal inhibitory neurons, which were randomly connected with a certain probability p. $p = 0$ indicates that the neurons make zero

synaptic contacts with other neurons, whereas $p = 1$ represents a fully connected network in which all neurons project on all other neurons (including themselves). The results presented in [Wang and Buzsáki, 1996] identify a critical number of synaptic contacts ($\simeq 40$) per neuron within a network, independently on the number of cells in the network, required for the emergence of synchronous activity. For 100 neurons, this would equate to a critical connection probability of $p = 0.4$. In our network, the connection probability was set to $p = 0.6$ so as to be higher than this critical probability, ensuring the presence of synchronous network activity.

2.4   External Current Stimulation

Throughout all our simulations, the network was stimulated with a constant current $I_{stim} = 0.4\,nA$. Heterogeneity was introduced in the form of Gaussian-distributed noise when initialising the resting potential and the synaptic conductance values of the neurons.

2.5   Model Parameters

Table 1 summarises the parameter values used for the hippocampal inhibitory neuron model, unless otherwise specified.

Table 1: Inhibitory neuron model parameters.

Parameter	Value
$\overline{g}_l$	$0.1\,mS\,cm^{-2}$
E_l	$-65\,mV$
$\overline{g}_K$	$9\,mS\,cm^{-2}$
E_K	$-90\,mV$
$\overline{g}_{Na}$	$35\,mS\,cm^{-2}$
E_{Na}	$55\,mV$
$area$	$14000\,\mu m^2$
C_m	$1\,\mu F\,cm^{-2}$
E_i	$-80\,mV$
τ_i	$10\,ms$

2.6   Network Synchronisation

The network synchronisation is computed using the coherence measure devised by [Wang and Buzsáki, 1996]. The measure computes the pair-wise co-occurrence of neuron action potentials $\kappa_{i,j}(\tau)$ given a time windows of size τ. For any pair of neurons X and Y, given their spike trains represented as a series of ones and zeroes depending on whether the neuron spiked or did not in the time window respectively:

$$X_i(l),\, Y_j(l) \in \{0, 1\}$$
$$l = 1, 2, ..., L \qquad L = \frac{t_{sim}}{\tau} \qquad \tau = 10\,ms$$

where $t_{sim} = 2000\,ms$ is the duration time of the simulation, and L is the number of time windows of size τ. Increasing the size of τ augments the probability of spike co-occurrence and allowing for larger synchronisation values which might be unrealistic. For all our computations

we used $\tau = 10\,ms$, which we deemed small enough to capture the dynamics of the network without compromising the reliability of the computed coherence values. The pair-wise coherence measure is quantified as:

$$\kappa_{i,j}(\tau) = \frac{\sum_{l=1}^{L} X_i(l) \cdot Y_j(l)}{\sqrt{\sum_{l=1}^{L} X_i(l) \cdot \sum_{l=1}^{L} Y_j(l)}}$$

The network synchronisation measure is then computed as the average $\kappa_{i,j}(\tau)$ for a randomly sampled subset of neuron pairs in the network:

$$\kappa(\tau) = \frac{\sum_{i,j \in P} \kappa_{i,j}(\tau)}{N}$$

where $P = \{(0,1), (3,4), ...\}$ is a subset of randomly sampled neuron pairs of size N. Unless otherwise specified, the network synchronisation is averaged over a subset containing 10% of the total neuron pairs in the network, without repetitions. $\kappa(\tau)$ is comprised between 0 and 1, representing an asynchronous population firing and fully synchronised firing respectively.

3   Results – Studying Tonic Inhibition

We began by studying the effects of propofol-mediated tonic inhibition on network oscillations. This was done by acting solely on the tonic conductance g_{ton}. The synaptic weight was fixed at $w_i = 1.6\,nS$, and the decay time constant was $\tau_i = 10\,ms$.

3.1   Tonic Inhibition Improves Neural Synchronisation

In the absence of anaesthetic agent ($g_{ton} = 0\,nS$), the network synchronised its activity with $\kappa(\tau) = 0.40$ (Figure 1a) at a population frequency of $f = 20.72\,Hz$ (Figure 1b), and an oscillatory frequency of $f_{osc} = 42.67\,Hz$ (Figure 1c). Increasing doses of propofol reduced the overall network activity and slowed down its oscillations, whilst the network synchronisation remained stable at an average value of $\overline{\kappa(\tau)} = 0.42 \pm 0.01$. When the tonic inhibition reached a critical value of $g_{ton} = 14\,nS$ at which the synchronisation increased abruptly reaching $\kappa(\tau) = 0.72$, and the mean firing rate increased to $f \simeq 18\,Hz$. The network synchronisation remained unchanged at an average plateau value of $\overline{\kappa(\tau)} = 0.76 \pm 0.00$ until further strengthening the effects of propofol $g_{ton} = 21\,nS$ caused the overall network activity to drastically decrease ($\kappa(\tau) = 0.02$, $f = 4.98\,Hz$ and $f_{osc} = 13.04\,Hz$), until it faded away ($\kappa(\tau) = 0$, $f = 0\,Hz$ and $f_{osc} = 0\,Hz$ for $g_{ton} \geq 21.5\,nS$).

Figure 2 shows the activity of the network for increasing values of g_{ton}, in the form of raster plots. Their corresponding computed LFP signals are shown in Figure 3. At $g_{ton} = 0\,nS$ the network displayed gamma frequency oscillations ($f_{osc} = 42.67\,Hz$) with an average population frequency of $f = 20.72\,Hz$ and a synchronisation of $\kappa(\tau) = 0.40$. This indicates that, on average, approximately half of the neurons fire synchronously at any given time, as shown in Figure 2a. In addition, each individual neuron fired once every two cycles. Taken together, these two observations indicate that the intrinsic firing rate of each isolated neuron was $f = 42.67\,Hz$, although the presence of synaptic inhibition halved it.

Increasing tonic inhibition above a threshold value of $14\,nS$ produced slower population firing rates, and slower oscillations. At $g_{ton} = 15\,nS$, the network activity oscillated at $f_{osc} = 20.67\,Hz$
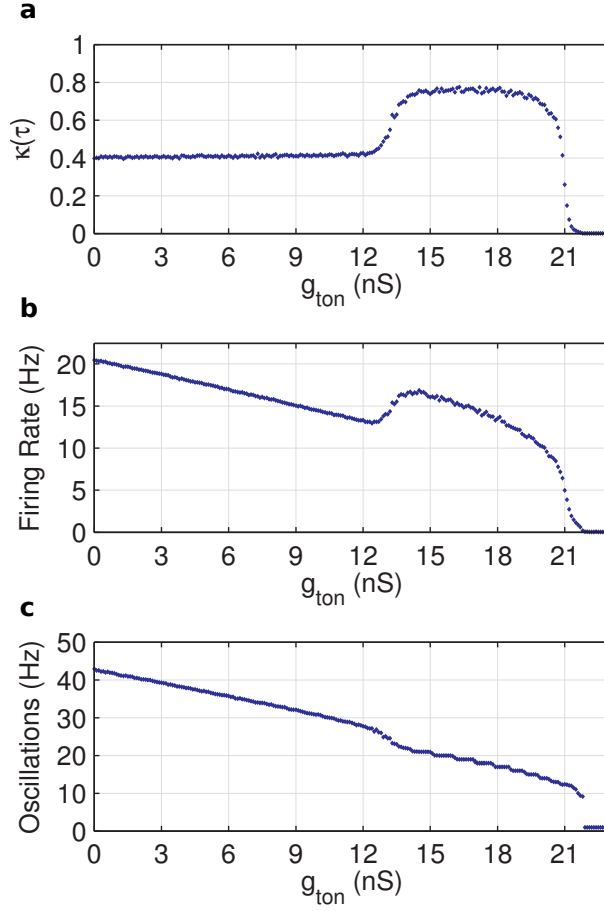
Figure 1: **Increasing propofol enhances network synchronisation. a** At low values of propofol ($0\,nS \leq g_{ton} \leq 13\,nS$) the network synchronisation is stable at an average value of $\overline{\kappa(\tau)} = 0.43 \pm 0.01$. Increasing the propofol dosage – by acting on the tonic conductance g_{ton} – causes the overall activity of the network to decrease, until a critical value of $g_{ton} = 14\,nS$ at which both the network synchronisation **a**, and the firing rate **b** increase to $\kappa(\tau) = 0.72$, and $f = 16.57\,Hz$ respectively. The oscillation frequency **c** follows a monotonically decelerating trend. When the concentration value reaches a value of $g_{ton} \geq 21.5\,nS$ the activity, synchronous or otherwise, fades out ($\kappa(\tau) = 0$, $f = 0\,Hz$ and $f_{osc} = 0\,Hz$ for $g_{ton} >= 21.5\,nS$).

with a population frequency of $f = 17.27\,Hz$ (Figure 2b). Similarly, at $g_{ton} = 18\,nS$, the network activity oscillated at $f_{osc} = 17.33\,Hz$ with a population frequency of $f = 14.08\,Hz$. (Figure 2c). We observe that, although slower, the oscillatory activity was approximately twice as synchronised $(\overline{\kappa(\tau)} = 0.76 \pm 0.00$ for $14\,nS \leq g_{ton} \leq 19\,nS)$ compared to the same network in the absence of tonic inhibition ($g_{ton} = 0\,nS$). As inhibition increased, the neurons in the network became less prone to discharging action potentials and the population frequency slowed down. In addition, stronger inhibition provided the neurons with tighter windows of increased excitability, ensuring that most of the neurons in the network (approximately 80%) would fire concurrently, which explains the enhanced network synchronisation.

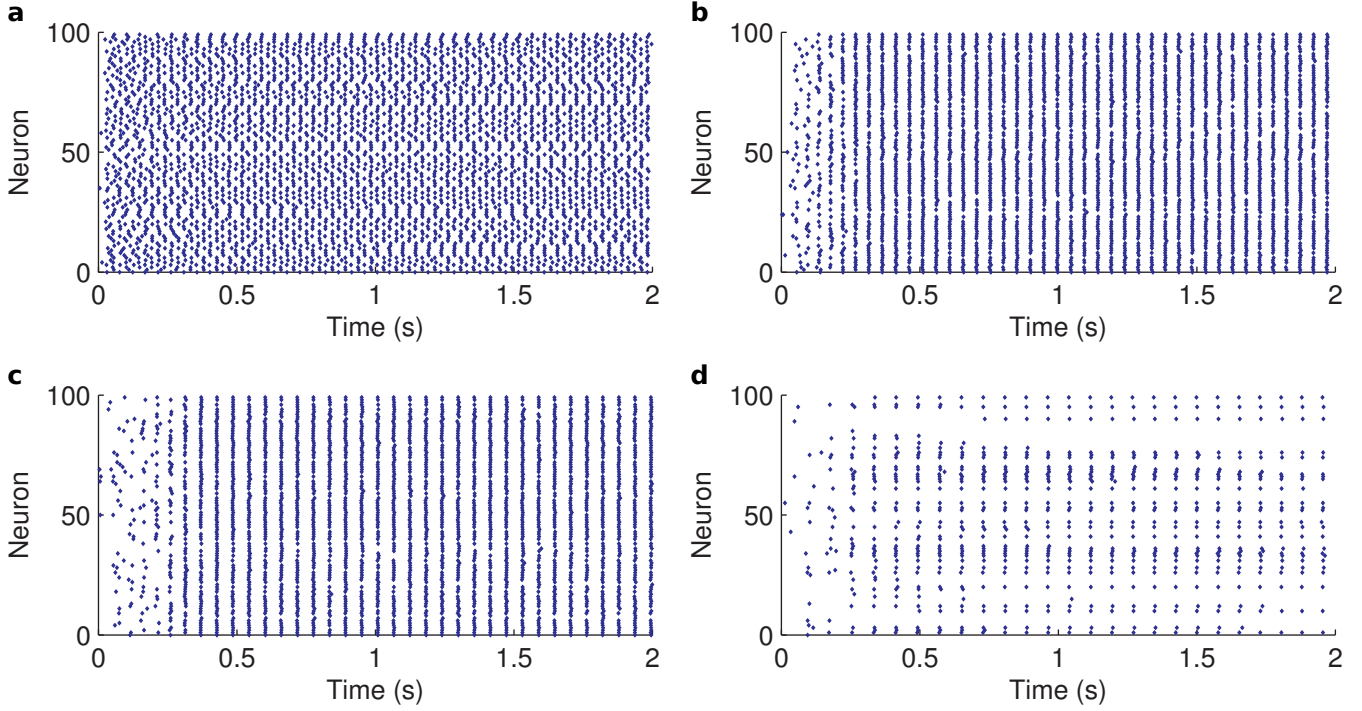Figure 2d shows weak, albeit synchronous activity at $f_{osc} = 12.67\,Hz$ with a population

Figure 2: **Increasing propofol dosage enhances network synchronisation. a** Raster plot for the 100-cell inhibitory network in the absence of propofol ($g_{ton} = 0\,nS$), showing $f_{osc} = 42.67\,Hz$ oscillations with a synchronisation of $\kappa(\tau) = 0.4$, $\tau = 10\,ms$. **b** Raster plot for the same network with a higher dose of propofol ($g_{ton} = 15\,nS$), showing $f_{osc} = 20.67\,Hz$ oscillations with a synchronisation of $\kappa(\tau) = 0.8$, $\tau = 10\,ms$. **c** Raster plot for the same network with a higher dose of propofol ($g_{ton} = 18\,nS$), showing $f_{osc} = 17.33\,Hz$ oscillations with a synchronisation of $\kappa(\tau) = 0.8$, $\tau = 10\,ms$. **d** Raster plot for the same network with a higher dose of propofol ($g_{ton} = 21\,nS$), showing $f_{osc} = 12.67\,Hz$ oscillations with a synchronisation of $\kappa(\tau) = 0.8$, $\tau = 10\,ms$. The network was stimulated with a constant current $I_{stim} = 0.4\,nA$.

frequency of $f = 3.85\,Hz$ for $g_{ton} = 21\,nS$. Further strengthening the tonic inhibition caused the neurons to emit fewer and fewer action potentials, until eventually the network activity faded away ($g_{ton} > 21\,nS$).

The LFP signal computed from the network activity reflected its synchronous behaviour (Figure 3). In the absence of propofol ($g_{ton} = 0\,nS$ in Figure 3a) the LFP oscillated between $-0.6\,mV$ and $0.7\,mV$ at $f_{osc} = 42.67\,Hz$. Increasing the effects of anaesthetics caused an increase in the amplitude of the LFP signal, which oscillated between $-1\,mV$ and $1.2\,mV$ at $f_{osc} = 20.67\,Hz$ for $g_{ton} = 15\,nS$ (Figure 3b), and $-0.95\,mV$ and $1.3\,mV$ at $f_{osc} = 17.33\,Hz$ for $g_{ton} = 18\,nS$ (Figure 3c). This increase in amplitude reflected the increase in network synchronisation as the more neurons fire concurrently at any given time the stronger the generated LFP signal will be. Similarly, the LFP amplitude decreased for $g_{ton} = 21\,nS$ (Figure 3d) as less neurons fire due to the strong tonic inhibition, producing an LFP signal which oscillated between $-0.32\,mV$ and $0.47\,mV$ at $f_{osc} = 12.67\,Hz$.

4 Results – Combining the Effects of Tonic and Phasic Inhibition

We then turned our attention towards analysing the joint effects of both synaptic and extrasynaptic propofol-enhanced inhibition. As previously explained, we modelled the action of propofol on synaptic $GABA_A$ receptors by increasing the inhibitory synaptic conductance, time constant, and current baseline. Our results show that solely the tonic inhibition was responsible for enhancing the network synchronisation in the presence of the anaesthetic agent.

4.1 Propofol-Enhanced Inhibitory Synaptic Conductance Does not Hinder Synchronisation

Increasing the inhibitory synaptic conductance did not hinder the synchronising properties of tonic inhibition (Figure 4). Figure 4a and Figure 4b depict the evolution of the average population frequency and synchronisation ($\kappa(\tau)$) respectively (vertical z axis), as both the synaptic weight w_i (y axis) and the tonic conductance g_{ton} (x axis) are increased, for a fixed synaptic time constant $\tau_i = 10\,ms$. Similarly, Figure 4c and Figure 4d illustrate the evolution of the average population frequency and synchronisation, for a fixed synaptic time constant $\tau_i = 14\,ms$. Finally, Figure 4e and Figure 4f show the evolution of the average population frequency and synchronisation, for a fixed synaptic time constant $\tau_i = 30\,ms$. The synaptic weights ranged between $1.4\,nS \leq w_i \leq 2.6\,nS$ and the tonic conductance ranged between $0\,nS \leq g_{ton} \leq 20\,nS$.

The overall population frequency decelerated from a maximum of $f = 21.97 \pm 0.06\,Hz$ to a minimum of $f = 7.78 \pm 0.25\,Hz$ as both w_i and g_{ton} grew (Figure 4a). However, whilst the firing rate followed a generally decreasing trend as synaptic weights were strengthened, it showed an up-and-down profile as tonic inhibition was enhanced, similar to that described previously in the absence of propofol-enhanced synaptic activity. Indeed, given $g_{ton} = 0\,nS$, the frequency slowed from $f = 21.97 \pm 0.06\,Hz$ for $w_i = 1.4\,nS$ to $f = 16.59 \pm 0.14\,Hz$ for $w_i = 2.6\,nS$. At $g_{ton} = 15\,nS$, the frequency slowed from $f = 16.81 \pm 0.18\,Hz$ for $w_i = 1.4\,nS$ to $f = 13.46 \pm 0.18\,Hz$ for $w_i = 2.6\,nS$. At $g_{ton} = 20\,nS$, the frequency slowed from $f = 10.53 \pm 0.26\,Hz$ for $w_i = 1.4\,nS$ to $f = 7.78 \pm 0.25\,Hz$ for $w_i = 2.6\,nS$. In contrast, we can observe a sharp increase in network frequency as tonic inhibition strengthens, given fixed synaptic weights. At $w_i = 1.4\,nS$, the frequency slowed from $f = 21.97 \pm 0.06\,Hz$ for $g_{ton} = 0\,nS$ to $f = 13.99 \pm 0.06\,Hz$ for $g_{ton} = 12\,nS$, then accelerated to $f = 16.81 \pm 0.18\,Hz$ for $g_{ton} = 15\,nS$, and finally dropped to $f = 10.53 \pm 0.26\,Hz$ for $g_{ton} = 20\,nS$. A similar bump pattern can be seen at all other values of w_i on Figure 4a. For example, at $w_i = 2.4\,nS$, the frequency slowed from $f = 17.08 \pm 0.12\,Hz$ for $g_{ton} = 0\,nS$ to $f = 13.08 \pm 0.35\,Hz$ for $g_{ton} = 10\,nS$, then accelerated to $f = 15.62 \pm 0.25\,Hz$ for $g_{ton} = 12\,nS$, and finally dropped to $f = 8.14 \pm 0.46\,Hz$ for $g_{ton} = 20\,nS$.

A similar trend can be observed, having fixed g_{ton}, on the evolution of the network synchronisation with respect to increasing values of w_i (Figure 4b). For example, at $g_{ton} = 0\,nS$, the synchronisation was $\kappa(\tau) = 0.34 \pm 0.02$ for $w_i = 1.4\,nS$, and $\kappa(\tau) = 0.36 \pm 0.01$ for $w_i = 2.6\,nS$, with a mean value of $\overline{\kappa(\tau)} = 0.36 \pm 0.00$. At $g_{ton} = 15\,nS$, the synchronisation was $\kappa(\tau) = 0.70 \pm 0.01$ for $w_i = 1.4\,nS$, and $\kappa(\tau) = 0.63 \pm 0.07$ for $w_i = 2.6\,nS$, with a mean value of $\overline{\kappa(\tau)} = 0.67 \pm 0.01$. At $g_{ton} = 20\,nS$, the synchronisation was $\kappa(\tau) = 0.65 \pm 0.01$ for $w_i = 1.4\,nS$, and $\kappa(\tau) = 0.48 \pm 0.04$ for $w_i = 2.6\,nS$, with a mean value of $\overline{\kappa(\tau)} = 0.59 \pm 0.01$. Comparing the stepwise synchronisation values with the average across all w_i values for a fixed g_{ton} indicated that synaptic inhibition accounts for little to no variability in the enhanced synchronous activity displayed by the network. Conversely, Figure 4b illustrates how the network synchronisation tightened for increasing values of g_{ton} given fixed synaptic weights, as previously observed (Figure 1a). At $w_i = 1.4\,nS$, the synchronisation remained stable at an average value of $\overline{\kappa(\tau)} = 0.37 \pm 0.01$ for $0\,nS \leq g_{ton} \leq 12\,nS$,

then increased to an average value of $\overline{\kappa(\tau)} = 0.65 \pm 0.04$ for $g_{ton} > 12\,nS$. This synchronisation bump pattern was preserved across all values of w_i. For example, at $w_i = 2.4\,nS$, the synchronisation stabilised at an average value of $\overline{\kappa(\tau)} = 0.36 \pm 0.01$ for $0\,nS \leq g_{ton} \leq 10\,nS$, then increased to an average value of $\overline{\kappa(\tau)} = 0.57 \pm 0.09$ for $g_{ton} > 10\,nS$.

In addition, we observed that stronger synaptic inhibition had a tendency to shift the tonic inhibition-mediated frequency rebound peak towards lower values of g_{ton}. Our results show that this seemed to be the sole effect of propofol-enhanced GABAergic phasic inhibition. For $1.4\,nS \leq w_i \leq 2\,nS$ the peak was centred around $g_{ton} = 15\,nS$, with a maximum frequency value of $16.81 \pm 0.18\,Hz$ (Figure 5a), and a corresponding coherence value of $\kappa(\tau) = 0.71 \pm 0.01$ (Figure 5b) at $w_i = 1.4\,nS$. Stronger synaptic weights ($w_i > 2\,nS$) moved the centre of the peak around $g_{ton} = 12\,nS$, with a maximum frequency value of $16.21 \pm 0.27\,Hz$ (Figure 5a), and a corresponding coherence value of $\kappa(\tau) = 0.63 \pm 0.02$ (Figure 5b) at $w_i = 2.1\,nS$. Likewise, the peak of the tonic inhibition-mediated synchronisation rebound was also affected by stronger synaptic activity. For $1.4\,nS \leq w_i \leq 2.4\,nS$ it remained centred around $g_{ton} = 15\,nS$, with a maximum coherence value of $\kappa(\tau) = 0.72 \pm 0.01$ (Figure 5b), and a corresponding frequency value of $16.66 \pm 0.21\,Hz$ (Figure 5a) at $w_i = 1.5\,nS$. Stronger synaptic weights ($w_i > 2.4\,nS$) moved the centre of the peak around $g_{ton} = 12\,nS$, with a maximum coherence value of $\kappa(\tau) = 0.63 \pm 0.01$ (Figure 5b), and a corresponding frequency value of $15.43 \pm 0.17\,Hz$ (Figure 5a) at $w_i = 2.6\,nS$. This behaviour is to be expected since the presence of stronger inhibition invariably caused a reduction in overall network activity thus producing slower firing rates.

4.2 Prolonged Synapse Closing Times Allow for Synchronisation with Weaker Tonic Inhibition

Propofol also enhances synaptic inhibitory currents by extending the closing time of the synapse [Bai et al., 2001, Kitamura et al., 2004, McDougall et al., 2008], allowing for longer lasting currents. We modelled this effect by prolonging the synaptic time constant τ_i. Figure 4a, Figure 4c and Figure 4e depict the relationship between the network frequency and the synaptic and tonic inhibition as τ_i is increased, from $10\,ms$ to $14\,ms$ to $30\,ms$ respectively. Intuitively, longer synaptic time constants should reduce the firing frequency of the network, as is reflected in our results. At $\tau_i = 10\,ms$ the maximum firing rate was $f = 21.97 \pm 1.24\,Hz$ for $w_i = 1.4\,nS$ and $g_{ton} = 0\,nS$ (Figure 4a). A longer time constant $\tau_i = 14\,ms$ decelerated the maximum firing rate to $f = 17.42 \pm 0.14\,Hz$ for $w_i = 1.4\,nS$ and $g_{ton} = 0\,nS$ (Figure 4c). Further extending τ_i to $14\,ms$ reduced the maximum firing rate to $f = 9.28 \pm 0.24\,Hz$ for $w_i = 1.4\,nS$ and $g_{ton} = 0\,nS$ (Figure 4e). In general, the network frequency was slower at all values of w_i and g_{ton} as τ_i was increased.

Longer synaptic time constants also affected the network synchronisation and its propofol-dependent bump-like evolution. Figure 4b, Figure 4d and Figure 4f depict the relationship between the network synchronisation and the synaptic and tonic inhibition as τ_i is increased, from $10\,ms$ to $14\,ms$ to $30\,ms$ respectively. Interestingly, we observe that extending the duration of the inhibitory synaptic current enhanced the network synchronisation at lower g_{ton} values, as longer time constants shifted the peak of the synchronisation bump towards the lower end of the x axis. At $\tau_i = 14\,ms$ (Figure 4d), given $w_i = 1.4nS$ the synchronisation stabilised at an average value of $\overline{\kappa(\tau)} = 0.29 \pm 0.01$ for $0\,nS \leq g_{ton} \leq 5\,nS$, then increased to an average value of $\overline{\kappa(\tau)} = 0.59 \pm 0.02$ for $5 < g_{ton} \leq 15\,nS$, and proceeded to drop to an average value of $\overline{\kappa(\tau)} = 0.31 \pm 0.01$ for $g_{ton} > 15\,nS$. Once again, this synchronisation bump pattern was preserved across all values of w_i. For example, a similar evolution can be observed at $w_i = 2.2\,nS$ where the synchronisation stabilised at an average value of $\overline{\kappa(\tau)} = 0.34 \pm 0.06$ for $0\,nS \leq g_{ton} \leq 5\,nS$, then increased to an average value of $\overline{\kappa(\tau)} = 0.41 \pm 0.02$ for $5 < g_{ton} \leq 15\,nS$, and proceeded to

drop to an average value of $\overline{\kappa(\tau)} = 0.18 \pm 0.02$ for $g_{ton} > 15\,nS$.

Further extending the synapse closing time caused further network frequency deceleration, as the number of spikes elicited were drastically reduced by the presence of stronger inhibition. Eventually, the network reverted to a slow, asynchronous firing regime. Figure 4e and Figure 4f illustrate the network frequency and synchronisation, respectively, for $\tau_i = 30\,ms$. The maximum frequency was reduced to $f = 9.28 \pm 0.24\,Hz$ for $w_i = 1.4\,nS$ and $g_{ton} = 0\,nS$. Whereas the maximum network synchronisation was reduced to $\kappa(\tau) = 0.18 \pm 0.01$. Both frequency and synchronisation followed decreasing trends as w_i and g_{ton} were increased, and the bump pattern was absent.

4.3 Tonic Inhibition-Mediated Synchronisation Is Unaffected by Potentiated Inhibitory Synaptic Baseline Currents

In vitro experimental studies [Jin et al., 2009, McDougall et al., 2008] have reported that exposure to propofol causes a concentration-dependent increase in GABAergic baseline currents in postsynaptic neurons. We modelled this effect by adding a constant $0\,pA \leq k_{bas} \leq 100\,pA$ to the inhibitory synaptic current I_i, where $k_{bas} = 0\,pA$ indicates the absence of propofol. To our knowledge, ours is the first computational study to include propofol-induced receptor desensitisation in its model. Our results indicate that a propofol-mediate shift in inhibitory synaptic baseline current does not interfere with the enhanced synchronisation provided by tonic inhibition. Figure 6 illustrates the relationship between the network frequency (vertical z axis) and the combined effects of tonic and synaptic inhibition – namely, increasing tonic conductance (x axis), shifting the inhibitory synaptic current baseline (y axis), enhancing synaptic current amplitudes (horizontally distributed surface plots), and prolonging synaptic current duration (vertically distributed surface plots). In particular, the top row of surface plots in Figure 6 depict the network frequency for $\tau_i = 10\,ms$ and increasing values of w_i i.e. $1.6\,nS$ (Figure 6a), $1.9\,nS$ (Figure 6b), and $1.9\,nS$ (Figure 6c) respectively. The middle row of surface plots in Figure 6 depict the network frequency for $\tau_i = 14\,ms$ and increasing values of w_i i.e. $1.6\,nS$ (Figure 6d), $1.9\,nS$ (Figure 6e), and $2.2\,nS$ (Figure 6f) respectively. The bottom row of surface plots in Figure 6 depict the network frequency for $\tau_i = 30\,ms$ and increasing values of w_i i.e. $1.6\,nS$ (Figure 6g), $1.9\,nS$ (Figure 6h), and $2.2\,nS$ (Figure 6i) respectively.

Similarly, Figure 7 illustrates the relationship between the network synchronisation (vertical z axis) and the combined effects of tonic and synaptic inhibition – namely, increasing tonic conductance (x axis), shifting the inhibitory synaptic current baseline (y axis), enhancing synaptic current amplitudes (horizontally distributed surface plots), and prolonging synaptic current duration (vertically distributed surface plots). In particular, the top row of surface plots in Figure 7 depict the network frequency for $\tau_i = 10\,ms$ and increasing values of w_i i.e. $1.6\,nS$ (Figure 7a), $1.9\,nS$ (Figure 7b), and $1.9\,nS$ (Figure 7c) respectively. The middle row of surface plots in Figure 7 depict the network frequency for $\tau_i = 14\,ms$ and increasing values of w_i i.e. $1.6\,nS$ (Figure 7d), $1.9\,nS$ (Figure 7e), and $2.2\,nS$ (Figure 7f) respectively. The bottom row of surface plots in Figure 7 depict the network frequency for $\tau_i = 30\,ms$ and increasing values of w_i i.e. $1.6\,nS$ (Figure 7g), $1.9\,nS$ (Figure 7h), and $2.2\,nS$ (Figure 7i) respectively.

The presence of a non-zero inhibitory baseline current had a general tendency to produce lower network firing rates. Indeed for $g_{ton} = 0\,nS$, $w_i = 1.6\,nS$, and $\tau_i = 10\,ms$, the network frequency was $20.83 \pm 0.07\,Hz$ at $k_{bas}0 = pA$, and decelerated to $16.76 \pm 0.07\,Hz$ at $k_{bas} = 100\,pA$. Moreover, for $g_{ton} = 20\,nS$, $w_i = 1.6\,nS$, and $\tau_i = 10\,ms$, the network frequency was $10.10 \pm 0.18\,Hz$ at $k_{bas}0 = pA$, and decelerated to $0.04 \pm 0.00\,Hz$ at $k_{bas} = 100\,pA$. However, the sharp acceleration of the network frequency caused by tonic inhibition remained unaffected, aside from increasing k_{bas} values causing the peak of the acceleration bump to shift towards lower

g_{ton} values. For example, in Figure 6a for $w_i = 1.6\,nS$, $\tau_i = 10\,ms$, and $k_{bas} = 0\,pA$ the peak of the acceleration was at $g_{ton} = 15\,nS$ with a frequency of $16.28 \pm 0.23\,Hz$. Increasing k_{bas} to $40\,pA$ shifted the peak to $g_{ton} = 12\,nS$ with a frequency of $15.73 \pm 0.25\,Hz$. Further increasing k_{bas} to $90\,pA$ shifted the peak to $g_{ton} = 10\,nS$ with a frequency of $15.26 \pm 0.17\,Hz$. This effect is comparable to that caused by stronger synaptic weights w_i, in that both increasing k_{bas} and w_i effectively correspond to an enhancement of global network inhibition.

As expected, longer synaptic time constants shifted the acceleration peak towards lower tonic inhibition strengths, regardless of the increasing synaptic baseline current. This shift can be observed when comparing the surface plots in Figure 6 vertically. Taking the first column of Figure 6 as an example, $w_i = 1.6\,nS$, $\tau_i = 10\,ms$, and $k_{bas} = 40\,pA$ the peak of the acceleration was at $g_{ton} = 15\,nS$ (Figure 6a). Extending the synaptic time constant to $\tau_i = 14\,ms$ shifts the peak to $g_{ton} = 5\,nS$ for $k_{bas} = 40\,pA$ (Figure 6d). A longer time constant $\tau_i = 30\,ms$ shifts the peak to $g_{ton} = 0\,nS$ for $k_{bas} = 40\,pA$ (Figure 6g). Finally, stronger inhibitory synaptic weights globally decelerated the network activity (Figure 6a, Figure 6b, and Figure 6c), whilst preserving the bump-like pattern in the population frequency. These behaviours are consistent with our previously reported findings within this Chapter.

In addition, the network tonic-inhibition mediated synchronisation seemed to remain unaffected as k_{bas} increased (Figure 7). The network continued to display enhanced synchronisation in the presence of critical degrees of tonic inhibition. Intensifying shifts in inhibitory baseline currents solely slightly shifted the synchronisation peak towards lower tonic conductance values. For example, in Figure 7a the synchronisation peak for $k_{bas} = 0\,pA$ was at $g_{ton} = 0\,nS$ with a synchronisation of $\kappa(\tau) = 0.70 \pm 0.01$ for $w_i = 1.6\,nS$, and $\tau_i = 10\,ms$. Increasing k_{bas} to $60\,pA$ shifted the peak to $g_{ton} = 12\,nS$ with a synchronisation of $\kappa(\tau) = 0.72 \pm 0.01$.

Longer synaptic time constants shifted the synchronisation peak towards lower tonic inhibition strengths, regardless of the increasing synaptic baseline current. This shift can be observed when comparing the surface plots in Figure 7 vertically. Finally, stronger inhibitory synaptic weights globally decreased the maximum attainable network synchronisation (Figure 7a, Figure 7b, and Figure 7c), whilst preserving the enhanced synchronisation phenomenon observed in the presence of tonic inhibition.

4.4 Tonic Inhibition Allows for the Emergence of Elevated Network Synchronisation

Having isolated the two model parameters which were responsible for significantly affecting the synchronisation exhibited by the network activity – namely, the tonic conductance g_{ton} and the synaptic time constant τ_i – we simulated an experiment in which we varied both of these parameters concurrently. The purpose of this simulation was to study the effect of the absorption of increasing doses of anaesthetic agent over time on network activity. We increased g_{ton} from $0\,nS$ to $20\,nS$ in steps of $2\,nS$, and τ_i from $10\,ms$ to $20\,ms$ in steps of $1\,ms$, in $2\,s$ intervals. Figure 8 depicts the raster plot of the network activity for the first $14\,s$ of simulation time, and Figure 9 the last $6\,s$ of simulation time. Each raster plot is divided into $6\,s$ intervals with an overlap of $2\,s$ between them i.e. Figure 8a shows the network spikes between $0\,s$ and $6\,s$, Figure 8b shows the network spikes between $4\,s$ and $10\,s$, Figure 8c shows the network spikes between $8\,s$ and $14\,s$, Figure 9d shows the network spikes between $12\,s$ and $18\,s$, and Figure 9e shows the network spikes between $16\,s$ and $22\,s$.

We observe how the network activity was fast ($\overline{f} = 18.79 \pm 0.03\,Hz$) but loosely synchronised ($\overline{\kappa(\tau)} = 0.41 \pm 0.01$) between $0\,s \leq t \leq 6\,s$ (Figure 8a), where $0\,nS \leq g_{ton} \leq 4\,nS$ and $10\,ms \leq \tau_i \leq 12\,ms$. During this period of time, the population frequency (Figure 10a) decelerated from $\overline{f} = 20.77 \pm 0.01\,Hz$ to $\overline{f} = 17.14 \pm 0.12\,Hz$, whilst the network synchronisation remained centred

around $\kappa(\tau) = 0.41 \pm 0.01$ (Figure 10b), as g_{ton} and τ_i increased (Figure 10c and Figure 10d respectively). As the neurons began absorbing stronger doses of propofol ($6\,nS \leq g_{ton} \leq 8\,nS$ and $13\,ms \leq \tau_i \leq 14\,ms$) tighter synchronous activity emerged increasing up to a maximum value of $\kappa(\tau) = 0.63 \pm 0.00$ for $g_{ton} = 8\,nS$ and $\tau_i = 14\,ms$. Concurrently, the network frequency accelerated to a maximum of $\overline{f} = 19.13 \pm 0.17\,Hz$ ($g_{ton} = 6\,nS$ and $\tau_i = 13\,ms$) and subsequently began decelerating. The enhanced synchronisation is reflected in the raster plots in Figure 8b showing its emergence at $t \simeq 6.5\,s$ and in Figure 8c illustrating how the synchronisation persisted.

$g_{ton} = 12\,nS$ and $\tau_i = 16\,ms$ at $t = 12\,s$ (Figure 9d) marked the end of the synchronisation rebound with $\kappa(\tau)$ decreasing from 0.63 ± 0.00 to 0.42 ± 0.00 and population frequency decelerating to $\overline{f} = 18.04 \pm 0.04\,Hz$. Finally, further increases in propofol dosage (Figure 9e) caused a gradual weakening of global network activity ($g_{ton} geq 14\,nS$, $\tau_i \geq 17\,ms$, and $t \geq 14\,s$), whose frequency eventually decayed to $\overline{f} = 2.74 \pm 0.02\,Hz$ with a synchronisation of $\kappa(\tau) = 0.08 \pm 0.00$ at $t = 22\,s$.

5   Conclusions and Discussion

GABAergic inhibition is thought to play an important role in the generation of oscillatory rhythmic activity in neural populations [Bartos et al., 2002, Bartos et al., 2007, Buzsáki and Wang, 2012, Cobb et al., 1995, Colgin, 2016]. In addition, GABA receptors have been shown to be the primary target of anaesthetic agents [Mueller et al., 2011, Rudolph and Antkowiak, 2004] and in particular of propofol [Vanlersberghe and Camu, 2008]. Indeed, propofol has been shown to target both synaptic and extrasynaptic GABA receptors with the effect of amplifying and extending the duration of inhibitory postsynaptic currents [Adodra and Hales, 1995, Bai et al., 2001, Kitamura et al., 2004, McDougall et al., 2008], enhancing extrasynaptic tonic inhibition [Bai et al., 2001, McDougall et al., 2008, Song et al., 2011], and slowing the receptor desensitisation [Bai et al., 1999, Bai et al., 2001, Jin et al., 2009, McDougall et al., 2008]. In this work we presented an in-depth study of the action of anaesthesia on neural oscillations by modelling all of the afore-mentioned effects on a network of hippocampal interneurons.

5.1   Tonic Inhibition Produces Tighter Synchronous Activity

Our results show how propofol-mediated tonic inhibition contributes to enhancing network synchronisation in a network of hippocampal interneurons. Whilst propofol does also act on the phasic inhibition mediated by synaptic $GABA_A$ receptors, neither the increase in the amplitude and duration of the synaptic response, nor the desensitisation due to propofol binding on these receptors seemed to account for an increase in network synchronisation. The sole significant effect of phasic inhibition was to lower the threshold of tonic conductance necessary for the emergence of enhanced network synchronisation, by prolonging the duration of inhibitory postsynaptic currents. Taken together, these observations allow us to conclude that the enhanced network synchronisation we observed was mostly dependent on tonic inhibition mediated by extrasynaptic GABA receptors.

5.2   Enhanced Synchronisation for Neuronal Communication under General Anaesthesia

The role of neural oscillations has been extensively described in the literature, giving rise to a number of stimulating theories. Neural oscillations may represent the stable, unperturbed state of the brain [Buzsáki and Draguhn, 2004] during sleep, and can also be used as indicators of certain sleep stages [Llinas and Ribary, 1993]. In addition, experimental studies

have linked synchronous activity with perception [Engel et al., 2001] stimulus encoding and representation [Gray et al., 1989], information integration and memory [Colgin and Moser, 2010, Engel et al., 2001, Kahana et al., 2001, Lisman, 2010, Lisman and Jensen, 2013, Varela et al., 2001] The common denominator of all of these theories is the hypothesis of neuronal communication through coherence [Fries, 2005], according to which synchronous activity enables communication and cooperation between neural ensembles. Indeed, functionally-linked brain regions have been shown to synchronise their operational frequency when collaborating. These include, and are not limited to, parietal and occipital regions during visual attention tasks [Fries et al., 2001]; hippocampus and (pre) frontal cortex during memory tasks [Fell et al., 2001] and consolidation during sleep [Maingret et al., 2016]; motor cortex and spinal motor neurons during movement tasks [Conway et al., 1995].

5.2.1 Intraoperative Awareness

The enhanced synchronisation described here could provide a possible mechanism supporting the occurrence of intraoperative awareness, intended as the explicit recollection of perceived stimuli during sedation. Patients who report having experienced intraoperative awareness often describe their ability to hear voices and sounds, to perceive visual stimuli such as the surgical lighting, to feel touch, and sometimes discomfort or pain [Ghoneim et al., 2009, Moerman et al., 1993, Ranta et al., 1998, Sandin et al., 2000, Schwender et al., 1998], accompanied by a feeling of helplessness and the inability to communicate. Although rarely occurring – 0.1% to 0.3% of patients according to experimental studies [Ghoneim et al., 2009, Jones, 1994, Ranta et al., 1998] which, if we consider that in the US alone approximately 60000 patients undergo general anaesthesia every day [Brown et al., 2010], equates to 60 to 180 patients per day –, intraoperative awareness is a traumatic experience which engenders fear and mistrust towards surgery and general anaesthesia, and can even sometimes lead to post-traumatic stress disorder [Osterman and Van Der Kolk, 1998, Osterman et al., 2001, Schwender et al., 1998]. The commons causes of intraoperative awareness are thought to be: insufficient drug dosages, increased anaesthetic requirements, damaged of defective drug delivery systems [Ghoneim et al., 2009, Mashour, 2010]. These findings indicate that the occurrence of intraoperative awareness is heavily dependent on the concentration of the anaesthetic agent administered to, and absorbed by, the patient.

General anaesthetics inhibit the conscious perception of pain but fail to fully cut off the pain transmission pathways from the sympathetic to the central nervous system. This is reflected in the haematological and metabolical responses commonly recorded under general anaesthesia, showing prototypical indicators of the surgical stress response – namely, increased heart rate and blood flow, and changes in skin conductance [Longnecker David E et al., 2008, Storm, 2008] – as well as in the statistical analyses of postoperative patient reports indicating that up to 30% of intraoperatively aware patients recall experiencing pain [Sebel et al., 2004]. Taken together, these observations indicate that the sympathetic and central nervous of system anaesthetised patients are capable of processing noxious stimuli. This allows us to postulate that propofol-enhanced network synchronisation could provide the favourable conditions needed for the perception of pain under general anaesthesia. Precise timing between the surgical incision and the anaesthesia-dependent improved synchronous activity could facilitate the transmission of pain stimuli to the central nervous system in anaesthetised patients.

5.2.2 Implicit Memory Formation

There is a large volume of published studies describing the formation of implicit memories under general anaesthesia [Andrade and Deeprose, 2007, Bonett et al., 2014, Cork et al., 1996,

Ghoneim and Block, 1997, Jones, 1994, Kihlstrom et al., 1990]. According to these, anaesthetised patients perceive and remember auditory stimuli, and are capable of recalling them in postoperative interviews, without being able to consciously identify when and how these stimuli were encoded. A recent study described how propofol enables a dose-dependent increase in synchronous activity within the human medio-temporal lobe under general anaesthesia [Fell et al., 2005]. These results, coupled with the theory that neural synchronisation between the entorhinal cortex and the hippocampus correlates with memory formation in humans [Fell et al., 2001], provide a possible neural substrate underlying mnemonic processes during anaesthesia. Our model supports this view by making the compelling prediction that anaesthetic agents could facilitate the communication between brain structures which should supposedly be not allowed to do so under general anaesthesia. Therefore, memory formation under general anaesthesia could be facilitated by a propofol-dependent enhancement in rhinal-hippocampal coherence.

The dosage-dependent synchronisation enhancement described here is a transient phenomenon that may depend on subject sensitivity. Moreover, its transient characteristics may render it hard to observe and monitor. This could explain why a recent study [Bejjani et al., 2009] did not find statistically significant evidence for implicit memory formation under general anaesthesia. A possible explanation could be that memory consolidation probably requires the conjunction of several conditions, for example a strong external stimulation (such as the noxious stimulus caused by a surgical incision) concurrent with the induction of anaesthesia. Indeed, it is not clear if memory formation happens during unconsciousness or during short periods of intraoperative awareness [Bailey and Jones, 1997, Bejjani et al., 2009, Deeprose et al., 2004, Kerssens et al., 2005, Lubke et al., 1999, Willems et al., 2005]. In addition, implicit memory formation could also depend on the interaction of anaesthetic agents with other perioperative drugs.

5.2.3   Paradoxical Excitation

Paradoxical excitation is a state of increased arousal which commonly occurs shortly during the initial phases of the induction of anaesthesia [Brown et al., 2010]. Although the mechanisms behind have been extensively investigated [Bevan et al., 1997, Clark and Rosner, 1973, Gibbs et al., 1936, Kiersey et al., 1951, McCarthy et al., 2008, Rampil, 1998], these are far from being fully unravelled. This phenomenon is dubbed "paradoxical" since it is caused by the administration of drugs which are supposed to suppress excitation rather than fostering it. Paradoxical excitation manifests itself in the form of involuntary purposeless or defensive movements, the expression of incoherent speech, and sometimes euphoria or dysphoria [Bevan et al., 1997, Clark and Rosner, 1973, Gibbs et al., 1936, Kiersey et al., 1951, McCarthy et al., 2008, Rampil, 1998].

One possible explanation behind the emergence of paradoxical excitation under general anaesthesia is based on the circuit hypothesis [Schiff and Posner, 2007, Schiff, 2008]. This theorises that a dosage-dependent disinhibition of striatothalamic pathways may allow the reactivation of stimuli which were temporarily stored within the thalamus prior to the induction of sedation. Since thalamocortical circuits have been shown to be involved in arousal regulation [Schiff, 2008] it is conceivable that a temporary stimulation of the thalamus could awaken anaesthetised subjects. Indeed, this was demonstrated to be the case in various experimental studies [Alkire et al., 2007, Schiff et al., 2007]. However, the mechanisms mediating this disinhibition under general anaesthesia remain unclear.

A theoretical model [McCarthy et al., 2008] attempted to provide another explanation for the occurrence of paradoxical excitation. Here, the authors investigated the cellular mechanisms underlying the changes in the EEG signal recorded from anaesthetised patients during paradoxical excitation events – namely an increase in beta power [Gugino et al., 2001]. Their results indicate that an interaction between the GABAergic synaptic current and an intrinsic

M-current produces a propofol-dependent switch in inhibitory network activity synchronisation, which enhances excitation in postsynaptic pyramidal neurons [McCarthy et al., 2008] leading to enhanced excitation. However, their model fails to account for the effects of propofol-mediated tonic inhibition. We suggest including these as an avenue for future work.

Acknowledgements

References

[Adodra and Hales, 1995] Adodra, S. and Hales, T. G. (1995). Potentiation, activation and blockade of GABAA receptors of clonal murine hypothalamic GT1-7 neurones by propofol. *British Journal of Pharmacology*, 115(6):953–960.

[Alkire et al., 2007] Alkire, M. T., McReynolds, J. R., Hahn, E. L., and Trivedi, A. N. (2007). Thalamic Microinjection of Nicotine Reverses Sevoflurane-induced Loss of Righting Reflex in the Rat. *Anesthesiology*, 107(2):264–272.

[Andrade and Deeprose, 2007] Andrade, J. and Deeprose, C. (2007). Unconscious memory formation during anaesthesia. *Best Practice & Research Clinical Anaesthesiology*, 21(3):385–401.

[Bai et al., 1999] Bai, D., Pennefather, P. S., MacDonald, J. F., and Orser, B. A. (1999). The general anesthetic propofol slows deactivation and desensitization of GABA(A) receptors. *The Journal of neuroscience : the official journal of the Society for Neuroscience*, 19(24):10635–10646.

[Bai et al., 2001] Bai, D., Zhu, G., Pennefather, P., Jackson, M. F., MacDonald, J. F., and Orser, B. A. (2001). Distinct functional and pharmacological properties of tonic and quantal inhibitory postsynaptic currents mediated by g -aminobutyric acid(A) receptors in hippocampal neurons. *Molecular Pharmacology*, 59(4):814–824.

[Bailey and Jones, 1997] Bailey, A. R. and Jones, J. G. (1997). Patients' memories of events during general anaesthesia. *Anaesthesia*, 52(5):460–476.

[Bartos et al., 2002] Bartos, M., Vida, I., Frotscher, M., Meyer, A., Monyer, H., Geiger, J. R. P., and Jonas, P. (2002). Fast synaptic inhibition promotes synchronized gamma oscillations in hippocampal interneuron networks. *Proceedings of the National Academy of Sciences of the United States of America*, 99(20):13222–13227.

[Bartos et al., 2007] Bartos, M., Vida, I., and Jonas, P. (2007). Synaptic mechanisms of synchronized gamma oscillations in inhibitory interneuron networks. *Nature reviews. Neuroscience*, 8(January):45–56.

[Bejjani et al., 2009] Bejjani, G., Lequeux, P.-Y., Schmartz, D., Engelman, E., and Barvais, L. (2009). No Evidence of Memory Processing During Propofol-Remifentanil Target-Controlled Infusion Anesthesia With Bispectral Index Monitoring in Cardiac Surgery. *Journal of Cardiothoracic and Vascular Anesthesia*, 23(2):175–181.

[Bevan et al., 1997] Bevan, J. C., Veall, G. R., Macnab, a. J., Ries, C. R., and Marsland, C. (1997). Midazolam premedication delays recovery after propofol without modifying involuntary movements. *Anesthesia and analgesia*, 85(1):50–4.

[Bonett et al., 2014] Bonett, E., Pham, X., Smith, K. R., Howard, K., Sheppard, S., and Davidson, A. (2014). Implicit memory formation using the word stem completion task during anesthesia in children. *Paediatric Anaesthesia*, 24(3):290–296.

[Brown et al., 2010] Brown, E. N., Lydic, R., and Schiff, N. D. (2010). General anesthesia, sleep, and coma. *The New England journal of medicine*, 363(27):2638–50.

[Buzsáki and Draguhn, 2004] Buzsáki, G. and Draguhn, A. (2004). Neuronal oscillations in cortical networks. *Science (New York, N.Y.)*, 304(5679):1926–9.

[Buzsáki and Wang, 2012] Buzsáki, G. and Wang, X.-J. (2012). Mechanisms of Gamma Oscillations. *Annual Review of Neuroscience*, 35(1):203–225.

[Clark and Rosner, 1973] Clark, D. L. and Rosner, B. S. (1973). Neurophysiologic effects of general anesthetics. I. The electroencephalogram and sensory evoked responses in man. *Anesthesiology*, 38(6):564–82.

[Cobb et al., 1995] Cobb, S. R., Buhl, E. H., Halasy, K., Paulsen, O., and Somogyi, P. (1995). Synchronization of neuronal activity in hippocampus by individual GABAergic interneurons. *Nature*, 378(6552):75–8.

[Colgin, 2016] Colgin, L. L. (2016). Rhythms of the hippocampal network. *Nature Reviews Neuroscience*.

[Colgin and Moser, 2010] Colgin, L. L. and Moser, E. I. (2010). Gamma oscillations in the hippocampus. *Physiology*, 25(5):319–29.

[Conway et al., 1995] Conway, B. A., Halliday, D. M., Farmer, S. F., Shahani, U., Maas, P., Weir, A. I., and Rosenberg, J. R. (1995). Synchronization between motor cortex and spinal motoneuronal pool during the performance of a maintained motor task in man. *Journal of Physiology*, 489(3):917–924.

[Cork et al., 1996] Cork, R. C., Heaton, J. F., Campbell, C. E., and Kihlstrom, J. F. (1996). Is there implicit memory after propofol sedation? *British journal of anaesthesia*, 76(4):492–8.

[Deeprose et al., 2004] Deeprose, C., Andrade, J., Varma, S., and Edwards, N. (2004). Unconscious learning during surgery with propofol anaesthesia. *British Journal of Anaesthesia*, 92(2):171–177.

[Engel et al., 2001] Engel, A. K., Fries, P., and Singer, W. (2001). Dynamic predictions: Oscillations and synchrony in top-down processing. *Nature Reviews Neuroscience*, 2(10):704–716.

[Fell et al., 2001] Fell, J., Klaver, P., Lehnertz, K., Grunwald, T., Schaller, C., Elger, C. E., and Fernández, G. (2001). Human memory formation is accompanied by rhinal-hippocampal coupling and decoupling. *Nature neuroscience*, 4(12):1259–64.

[Fell et al., 2005] Fell, J., Widman, G., Rehberg, B., Elger, C. E., and Fernández, G. (2005). Human mediotemporal EEG characteristics during propofol anesthesia. *Biological cybernetics*, 92(2):92–100.

[Fries, 2005] Fries, P. (2005). A mechanism for cognitive dynamics: neuronal communication through neuronal coherence. *Trends in cognitive sciences*, 9(10):474–80.

[Fries et al., 2001] Fries, P., Reynolds, J. R., Rorie, A. E., and Robert, D. (2001). Modulation of Oscillatory Neuronal Synchronization by Selective Visual Attention. *Science*, 291(5508):1560–1563.

[Garcia et al., 2010] Garcia, P. S., Kolesky, S. E., and Jenkins, A. (2010). General anesthetic actions on GABA(A) receptors. *Current neuropharmacology*, 8(1):2–9.

[Ghoneim and Block, 1997] Ghoneim, M. M. and Block, R. I. (1997). Learning and Memory during General Anesthesia An Update. *Anesthesiology*, 87:387–410.

[Ghoneim et al., 2009] Ghoneim, M. M., Block, R. I., Haffarnan, M., and Mathews, M. J. (2009). Awareness during anesthesia: Risk factors, causes and sequelae: A review of reported cases in the literature. *Anesthesia and Analgesia*, 108(2):527–535.

[Gibbs et al., 1936] Gibbs, F. A., Gibbs, E. L., and Lennox, W. G. (1936). Effect on the electro-encephalogram of certain drugs which influence nervous activity. *Archives of Internal Medicine*, 60(1):154–166.

[Gray et al., 1989] Gray, C. M., König, P., Engel, A. K., and Singer, W. (1989). Oscillatory responses in cat visual cortex exhibit inter-columnar synchronization which reflects global stimulus properties.

[Gugino et al., 2001] Gugino, L. D., Chabot, R. J., Prichep, L. S., John, E. R., Formanek, V., and Aglio, L. S. (2001). Quantitative EEG changes associated with loss and return of consciousness in healthy adult volunteers anaesthetized with propofol or sevoflurane. *British Journal of Anaesthesia*, 87(3):421–428.

[Hutt and Buhry, 2014] Hutt, A. and Buhry, L. (2014). Study of GABAergic extra-synaptic tonic inhibition in single neurons and neural populations by traversing neural scales: application to propofol-induced anaesthesia. *Journal of computational neuroscience*, 37(3):417–37.

[Jin et al., 2009] Jin, Y. H., Zhang, Z., Mendelowitz, D., and Andresen, M. C. (2009). Presy-naptic actions of propofol enhance inhibitory synaptic transmission in isolated solitary tract nucleus neurons. *Brain Research*, 1286:75–83.

[Jonas et al., 2004] Jonas, P., Bischofberger, J., Fricker, D., and Miles, R. (2004). Interneuron Diversity series: Fast in, fast out - Temporal and spatial signal processing in hippocampal interneurons. *Trends in Neurosciences*, 27(1):30–40.

[Jones, 1994] Jones, J. G. (1994). Perception and memory during general anaesthesia. *British Journal of Anaesthesia*, 73(1):31–37.

[Kahana et al., 2001] Kahana, M. J., Seelig, D., and Madsen, J. R. (2001). Theta returns. *Current Opinion in Neurobiology*, 11(6):739–744.

[Kerssens et al., 2005] Kerssens, C., Ouchi, T., and Sebel, P. S. (2005). No Evidence of Memory Function during Anesthesia with Propofol or Isoflurane with Close Control of Hypnotic State. *Anesthesiology*, 102(1):57–62.

[Kiersey et al., 1951] Kiersey, D. K., Bickford, R. G., and Faulconer, A. (1951). Electro-encephalographic patterns produced by thiopental sodium during surgical operations: Description and classification. *British Journal of Anaesthesia*, 23(3):141–152.

[Kihlstrom et al., 1990] Kihlstrom, J. F., Schacter, D. L., Cork, R. C., Hurt, C. a., and Behr, S. E. (1990). Implicit and Explicit Memory Following Surgical Anesthesia. *Psychological Science*, 1(5):303–306.

[Kitamura et al., 2004] Kitamura, A., Sato, R., Marszalec, W., Yeh, J. Z., Ogawa, R., and Narahashi, T. (2004). Halothane and propofol modulation of gamma-aminobutyric acidA receptor single-channel currents. *Anesthesia and analgesia*, 99(2):409–15, table of contents.

[Kopell et al., 2010] Kopell, N. J., Boergers, C., Pervouchine, D., Malerba, P., and Tort, A. (2010). Gamma and theta rhythms in biophysical models of hippocampal circuits. In Cutsuridis, V., Graham, B., Cobb, S., and Vida, I., editors, *Hippocampal Microcircuits A Computational Modeler's Resource Book*, chapter Gamma and, pages 423–457. Springer New York, New York, NY.

[Lisman, 2010] Lisman, J. E. (2010). Working memory: The importance of theta and gamma oscillations. *Current Biology*, 20(11):R490–R492.

[Lisman and Jensen, 2013] Lisman, J. E. and Jensen, O. (2013). The Theta-Gamma Neural Code. *Neuron*, 77(6):1002–1016.

[Llinas and Ribary, 1993] Llinas, R. and Ribary, U. (1993). Coherent 40-Hz oscillation characterizes dream state in humans. *Proceedings of the National Academy of Sciences*, 90(5):2078–2081.

[Longnecker David E et al., 2008] Longnecker David E, Brown, D. L., Newman, M. F., and Zapol, W. M. (2008). *Anesthesiology*. McGraw-Hill.

[Lubke et al., 1999] Lubke, G. H., Kerssens, C., Phaf, H., and Sebel, P. S. (1999). Dependence of explicit and implicit memory on hypnotic state in trauma patients. *Anesthesiology*, 90:670–680.

[Maingret et al., 2016] Maingret, N., Girardeau, G., Todorova, R., Goutierre, M., and Zugaro, M. (2016). Hippocampo-cortical coupling mediates memory consolidation during sleep. *Nature Neuroscience*, 19:959–964.

[Mashour, 2010] Mashour, G. A., editor (2010). *Consciousness, Awareness, and Anesthesia*. Cambridge University Press.

[McCarthy et al., 2008] McCarthy, M. M., Brown, E. N., and Kopell, N. J. (2008). Potential network mechanisms mediating electroencephalographic beta rhythm changes during propofol-induced paradoxical excitation. *The Journal of neuroscience : the official journal of the Society for Neuroscience*, 28(50):13488–13504.

[McDougall et al., 2008] McDougall, S. J., Bailey, T. W., Mendelowitz, D., and Andresen, M. C. (2008). Propofol enhances both tonic and phasic inhibitory currents in second-order neurons of the solitary tract nucleus (NTS). *Neuropharmacology*, 54(3):552–563.

[Moerman et al., 1993] Moerman, N., Bonke, B., and Oosting, J. (1993). Awareness and recall during general anesthesia: Facts and feelings. *Anesthesiology*, 79:454–464.

[Mueller et al., 2011] Mueller, C. P., Pum, M. E., Amato, D., Schüttler, J., Huston, J. P., and Silva, M. a. D. S. (2011). The in vivo neurochemistry of the brain during general anesthesia. *Journal of neurochemistry*, 119(3):419–46.

[Nelson et al., 2002] Nelson, L. E., Guo, T. Z., Lu, J., Saper, C. B., Franks, N. P., and Maze, M. (2002). The sedative component of anesthesia is mediated by GABA(A) receptors in an endogenous sleep pathway. *Nature neuroscience*, 5(10):979–84.

[Osterman et al., 2001] Osterman, J. E., Hopper, J., Heran, W. J., Keane, T. M., and Van Der Kolk, B. A. (2001). Awareness under anesthesia and the development of posttraumatic stress disorder. *General hospital psychiatry*, 23:198–204.

[Osterman and Van Der Kolk, 1998] Osterman, J. E. and Van Der Kolk, B. A. (1998). Awareness during anesthesia and posttraumatic stress disorder. *General hospital psychiatry*, 20(5):274–81.

[Rampil, 1998] Rampil, I. J. (1998). A primer for EEG signal processing in anesthesia. *The Journal of the American Society of Anesthesiologists*, 89(4):980–1002.

[Ranta et al., 1998] Ranta, S. O.-V., Laurila, R., Saario, J., Ali-Melkkila, T., and Hynynen, M. (1998). Awareness with Recall During General Anesthesia. *Anesthesia & Analgesia*, 86(5):1084–1089.

[Rinzel and Ermentrout, 1998] Rinzel, J. and Ermentrout, B. (1998). Analysis of neural excitability and oscillations. *Methods in neuronal modeling*, 2:251–292.

[Rudolph and Antkowiak, 2004] Rudolph, U. and Antkowiak, B. (2004). Molecular and neuronal substrates for general anaesthetics. *Nature reviews. Neuroscience*, 5(9):709–20.

[Sandin et al., 2000] Sandin, R. H., Enlund, Gunnar, Samuelsson, P., and Lennmarken, C. (2000). Awareness during anaesthesia. A prospective study. *The Lancet*, 355:707–711.

[Schiff, 2008] Schiff, N. D. (2008). Central thalamic contributions to arousal regulation and neurological disorders of consciousness. *Annals of the New York Academy of Sciences*, 1129:105–118.

[Schiff et al., 2007] Schiff, N. D., Giacino, J. T., Kalmar, K., Victor, J. D., Baker, K., Gerber, M., Fritz, B., Eisenberg, B., O'Connor, J., Kobylarz, E. J., Farris, S., Machado, A., McCagg, C., Plum, F., Fins, J. J., and Rezai, A. R. (2007). Behavioural improvements with thalamic stimulation after severe traumatic brain injury. *Nature*, 448(7153):600–603.

[Schiff and Posner, 2007] Schiff, N. D. and Posner, J. B. (2007). Another "Awakenings". *Annals of Neurology*, 62(1):5–7.

[Schwender et al., 1998] Schwender, D., Kunze-Kronawitter, H., Dietrich, P., Klasing, S., Forst, H., and Madler, C. (1998). Conscious awareness during general anaesthesia: patients' perceptions, emotions, cognition and reactions. *British Journal of Anaesthesia*, 80(2):133–139.

[Sebel et al., 2004] Sebel, P. S., Bowdle, T. A., Ghoneim, M. M., Rampil, I. J., Padilla, R. E., Gan, T. J., and Domino, K. B. (2004). The incidence of awareness during anesthesia: a multicenter United States study. *Anesthesia and analgesia*, 99(3):833–9, table of contents.

[Song et al., 2011] Song, I., Savtchenko, L., and Semyanov, A. (2011). Tonic excitation or inhibition is set by GABA(A) conductance in hippocampal interneurons. *Nature communications*, 2:376.

[Storm, 2008] Storm, H. (2008). Changes in skin conductance as a tool to monitor nociceptive stimulation and pain. *Current Opinion in Anaesthesiology*, 21(6):796–804.

[Vanlersberghe and Camu, 2008] Vanlersberghe, C. and Camu, F. (2008). Propofol. In Schüttler, J. and Schwilden, H., editors, *Modern Anesthetics: Handbook of Experimental Pharmacology*, pages 227–252. Springer Verlag.

[Varela et al., 2001] Varela, F., Lachaux, J. P., Rodriguez, E., and Martinerie, J. (2001). The brainweb: phase synchronization and large-scale integration. *Nature reviews. Neuroscience*, 2(4):229–39.

[Wang and Buzsáki, 1996] Wang, X.-J. and Buzsáki, G. (1996). Gamma oscillation by synaptic inhibition in a hippocampal interneuronal network model. *The Journal of Neuroscience : the official journal of the Society for Neuroscience*, 16(20):6402–13.

[Willems et al., 2005] Willems, S. J., Forster, A., and Linden, M. V. D. (2005). Investigation of Implicit Memory during Isoflurane Anesthesia for Elective Surgery Using the Process. *Anesthesiology*, 103:925–933.

[Zhou et al., 2012] Zhou, C., Liu, J., and Chen, X.-D. (2012). General anesthesia mediated by effects on ion channels. *World journal of critical care medicine*, 1(3):80–93.

Contents

Figure 3: **The synchronous activity displayed by the interneuron network is reflected in the computed LFP signals. a** LFP signal computed from the spiking activity of the inhibitory network in the absence of propofol shows $f_{osc} = 42.67\,Hz$ oscillations with a synchronisation of $\kappa(\tau) = 0.4$, $\tau = 10\,ms$ (one-second extract). **b** LFP signal computed from the spiking activity of the inhibitory network with a higher dose of propofol ($g_{ton} = 15\,nS$), showing $f_{osc} = 20.67\,Hz$ oscillations with a synchronisation of $\kappa(\tau) = 0.8$, $\tau = 10\,ms$ (one-second extract). **c** LFP signal computed from the spiking activity of the inhibitory network with a higher dose of propofol ($g_{ton} = 18\,nS$), showing $f_{osc} = 17.33\,Hz$ oscillations with a synchronisation of $\kappa(\tau) = 0.8$, $\tau = 10\,ms$ (one-second extract). **d** LFP signal computed from the spiking activity of the inhibitory network with a higher dose of propofol ($g_{ton} = 21\,nS$), showing $f_{osc} = 12.67\,Hz$ oscillations with a synchronisation of $\kappa(\tau) = 0.8$, $\tau = 10\,ms$ (one-second extract).
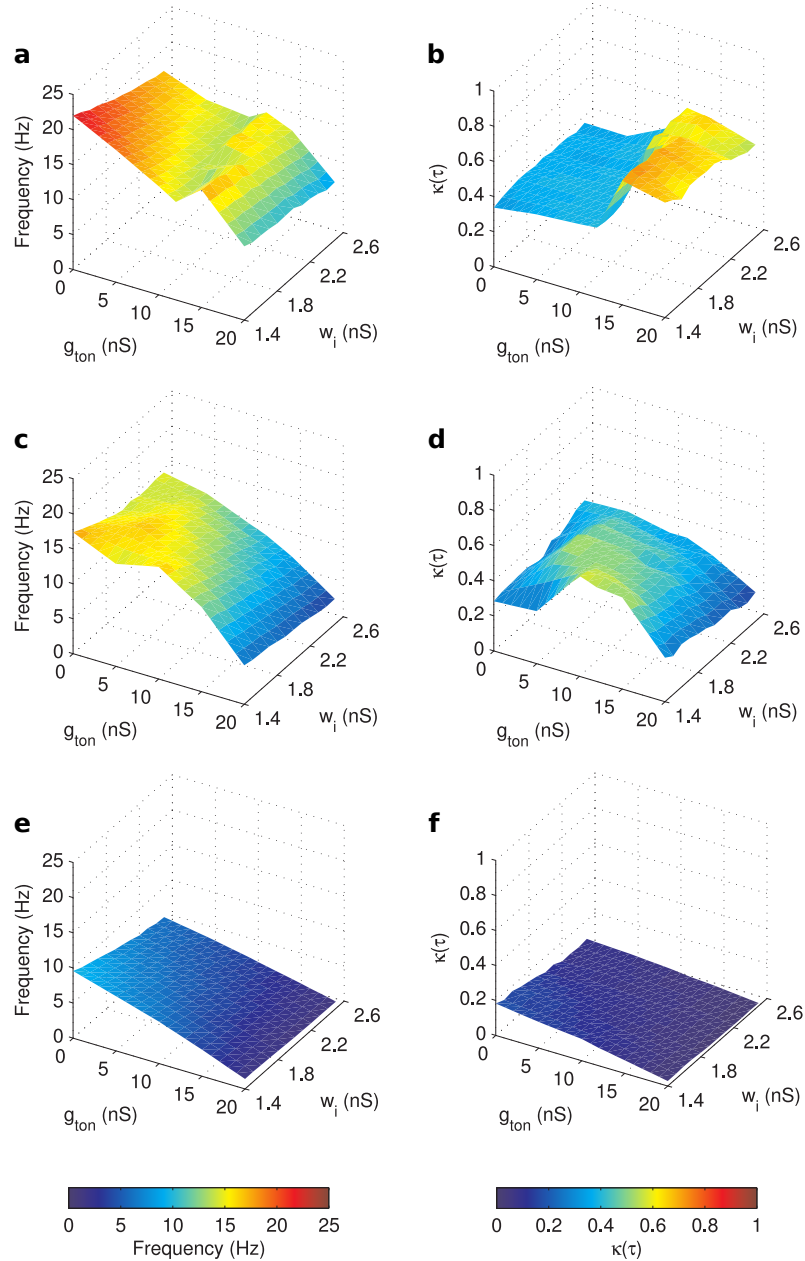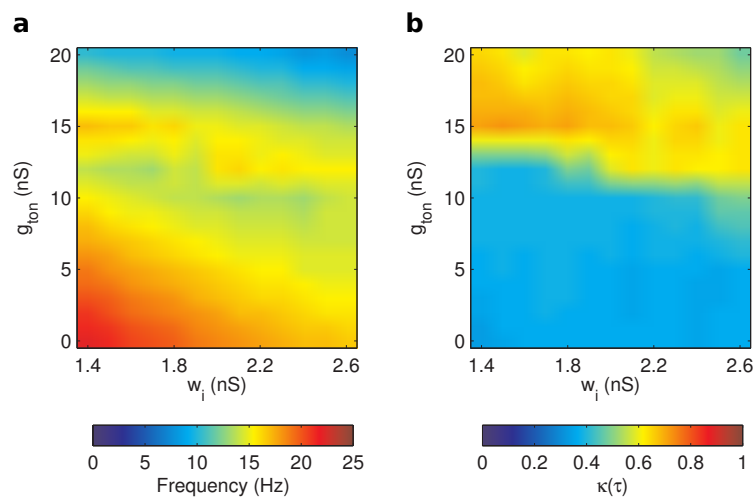
Figure 4: **Propofol-enhanced tonic inhibition allows for tighter network synchronisation, regardless of the presence of stronger inhibitory synapses.** In all the plots, the x axis represents the tonic conductance (g_{ton}) and the y axis represents the inhibitory synaptic weight (w_i). **a** Given $\tau_i = 10\,ms$, the network frequency decelerates as tonic inhibition strengthens until a critical value at which it accelerates. **b** This acceleration is due to an abrupt increase in network synchronisation at $g_{ton} \geq 15\,nS$ for all values of w_i. **c** A longer synaptic time constant ($\tau_i = 14\,ms$) shifts the network frequency bump towards lower values of g_{ton}. **d** Similarly, the network synchronisation bump shifts towards lower values of g_{ton}. **e** Extending the synaptic time constant ($\tau_i = 30\,ms$) causes the bump-like pattern of the network frequency to disappear in favour of a linearly decelerating trend. **f** Similarly, the bump-like pattern of the network synchronisation disappears in favour of a linearly decelerating trend. The network was stimulated with a constant current $I_{stim} = 0.4\,nA$.

Figure 5: **Propofol-enhanced tonic inhibition allows for tighter network synchronisation, regardless of the presence of stronger inhibitory synapses. a** Increasing tonic inhibition (y axis) causes an abrupt acceleration at $g_{ton} = 15\,nS$. The sole effect of synaptic inhibition (x axis) is to shift the peak of the acceleration towards lower g_{ton} values. **b** Similarly, tonic inhibition causes an abrupt enhanced synchronisation, whose peak is shifted towards lower g_{ton} values as w_i increases. The network was stimulated with a constant current $I_{stim} = 0.4\,nA$.
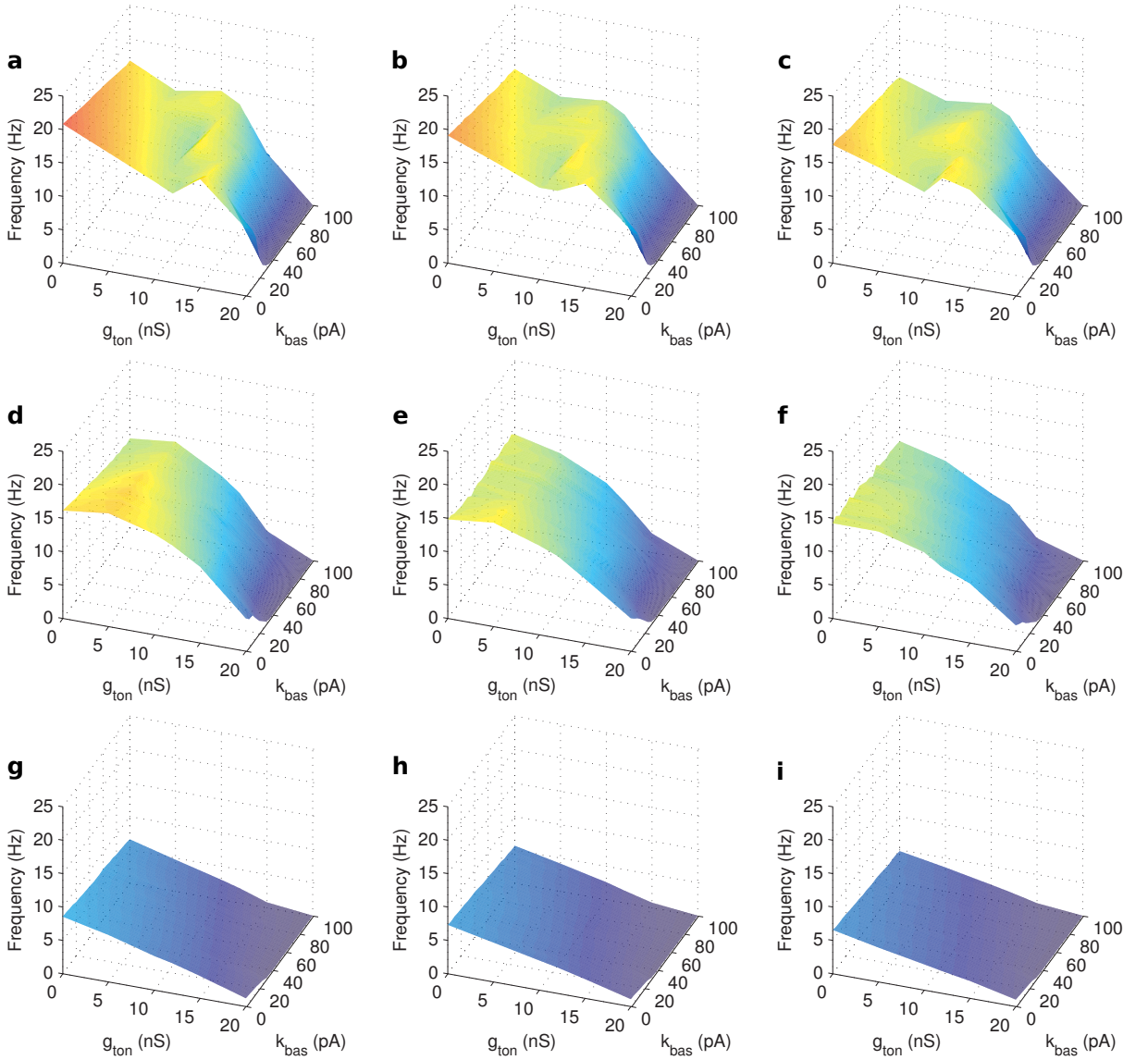
Figure 6: **Propofol-enhanced tonic inhibition decelerates the population firing rate, regardless of the presence of a stronger inhibitory baseline current.** **a** Given $\tau_i = 10\,ms$ and $w_i = 1.6\,nS$, the bump-like pattern caused by the tonic inhibition-mediated (x axis) deceleration followed by an acceleration of the network frequency is unaffected by the presence of a non-zero synaptic baseline current (y axis). These only slightly shift the peak of the acceleration towards lower g_{ton} values. The acceleration bump is unaffected by stronger synaptic weights – $w_i = 1.9\,nS$ in **b**, and $w_i = 1.6\,nS$ in **c**. **d** Given $\tau_i = 14\,ms$ and $w_i = 1.6\,nS$, the peak of the acceleration shifts towards lower g_{ton} values. This behaviour is unaffected by stronger synaptic weights – $w_i = 1.9\,nS$ in **e**, and $w_i = 1.6\,nS$ in **f**. **g** Given $\tau_i = 30\,ms$ and $w_i = 1.6\,nS$, the network acceleration follows a decreasing trend as g_{ton} and k_{bas} are increased. This behaviour is unaffected by stronger synaptic weights – $w_i = 1.9\,nS$ in **h**, and $w_i = 1.6\,nS$ in **i**. The network was stimulated with a constant current $I_{stim} = 0.4\,nA$.
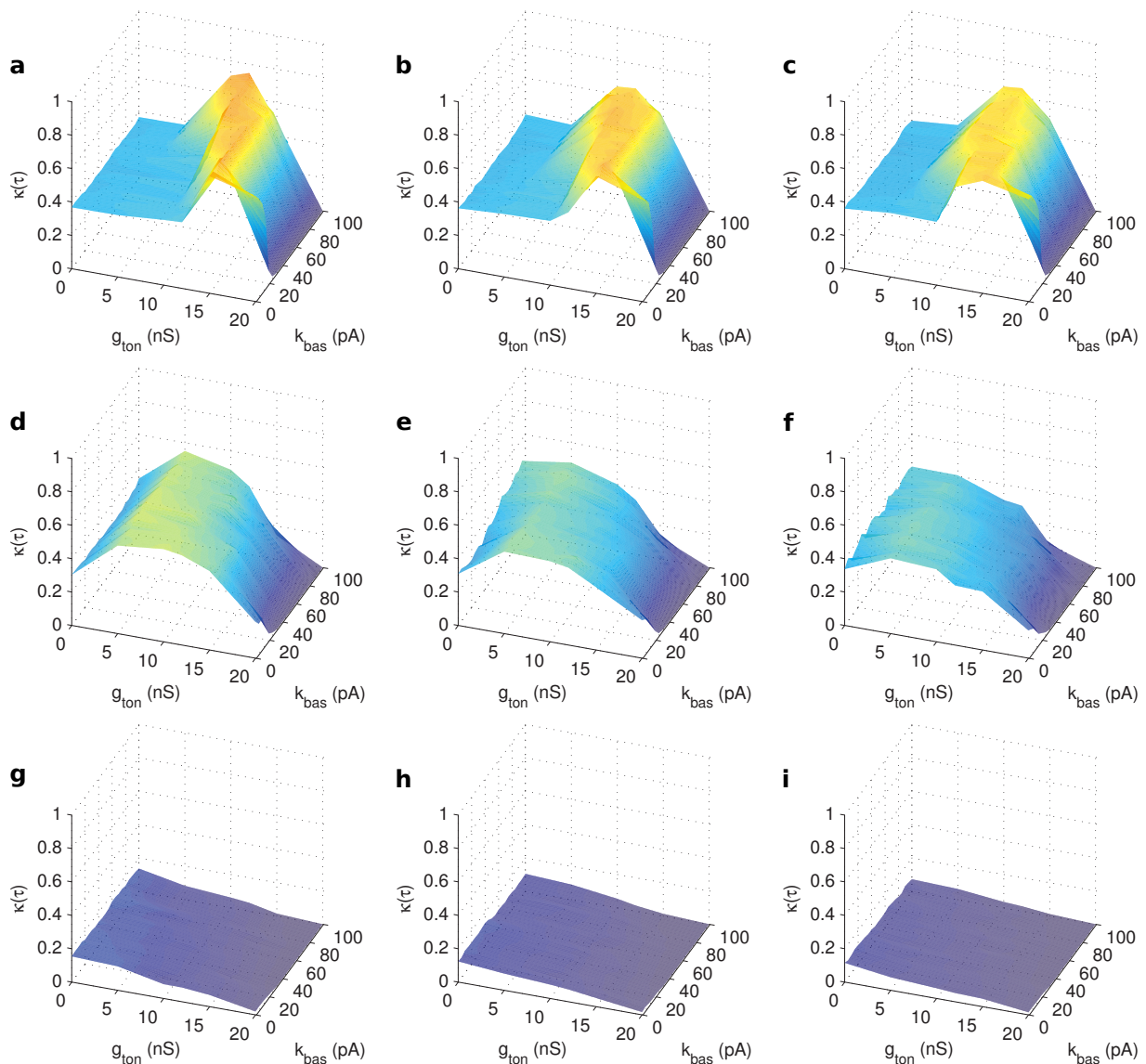
Figure 7: **Propofol-enhanced tonic inhibition allows for tighter network synchronisation, regardless of the presence of a stronger inhibitory baseline current. a** Given $\tau_i = 10\,ms$ and $w_i = 1.6\,nS$, the bump-like pattern caused by the tonic inhibition-mediated (x axis) enhanced synchronisation is unaffected by the presence of a non-zero synaptic baseline current (y axis). These only slightly shift the peak of the synchronisation towards lower g_{ton} values. The synchronisation bump is unaffected by stronger synaptic weights – $w_i = 1.9\,nS$ in **b**, and $w_i = 1.6\,nS$ in **c**. **d** Given $\tau_i = 14\,ms$ and $w_i = 1.6\,nS$, the peak of the synchronisation shifts towards lower g_{ton} values. This behaviour is unaffected by stronger synaptic weights – $w_i = 1.9\,nS$ in **e**, and $w_i = 1.6\,nS$ in **f**. **g** Given $\tau_i = 30\,ms$ and $w_i = 1.6\,nS$, the network synchronisation follows a decreasing trend as g_{ton} and k_{bas} are increased. This behaviour is unaffected by stronger synaptic weights – $w_i = 1.9\,nS$ in **h**, and $w_i = 1.6\,nS$ in **i**. The network was stimulated with a constant current $I_{stim} = 0.4\,nA$.
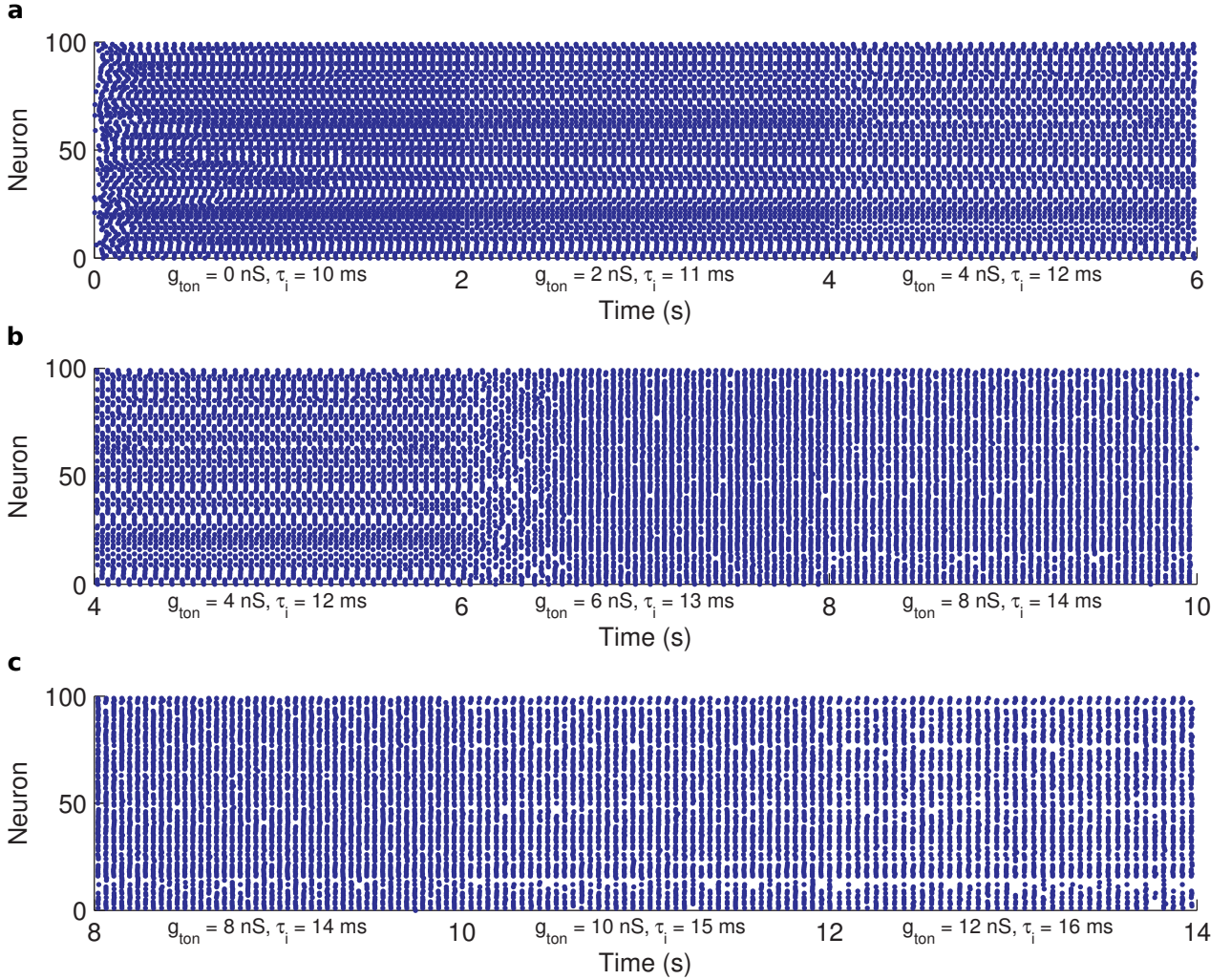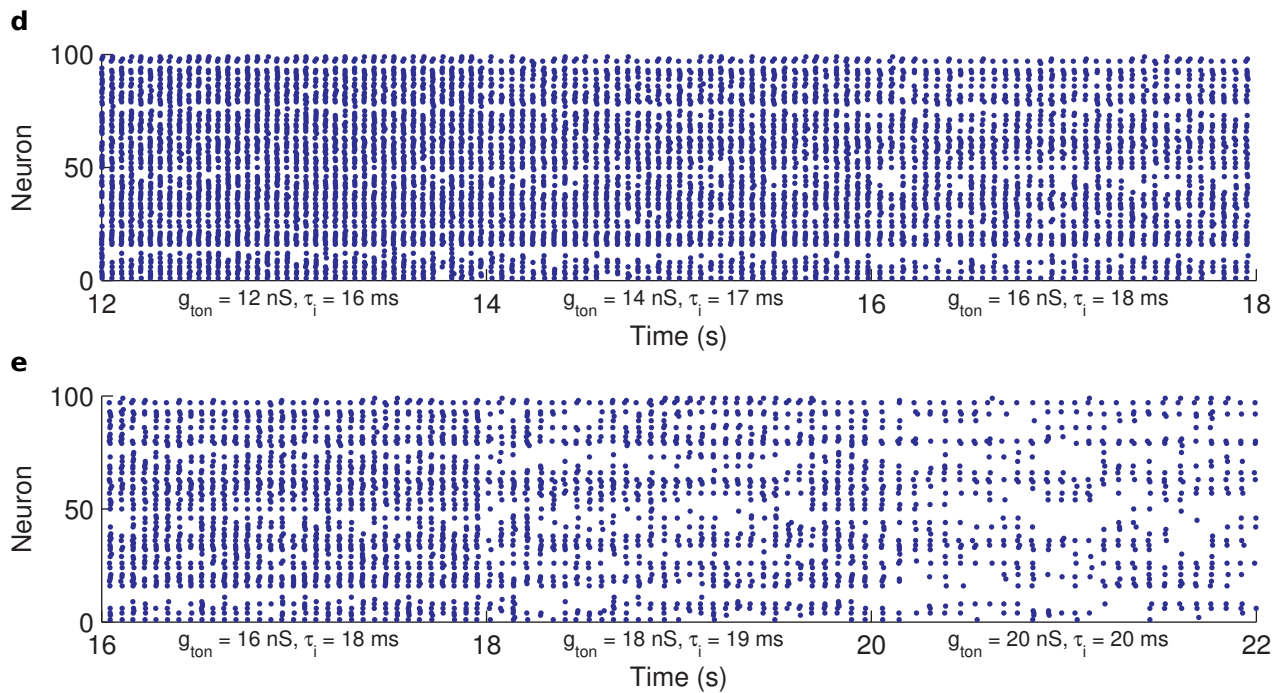
Figure 8: **Enhanced network synchronisation emerges as tonic inhibition is strengthened and synaptic time constants are prolonged.** g_{ton} and τ_i are increased every $2\,s$ in steps of $2\,nS$ and $1\,ms$ respectively. **a** Initially the network activity is fast $(\overline{f} = 18.79 \pm 0.03\,Hz)$ but loosely synchronised $(\overline{\kappa(\tau)} = 0.41 \pm 0.01)$ between $0\,s \leq t \leq 6\,s$, where $0\,nS \leq g_{ton} \leq 4\,nS$ and $10\,ms \leq \tau_i \leq 12\,ms$. **b** Enhanced synchronisation emerges at $t \simeq 6.5\,ms$, and the network activity accelerates to a maximum of $\overline{f} = 19.13 \pm 0.17\,Hz$ for $g_{ton} = 6\,nS$ and $\tau_i = 13\,ms$. **c** The maximum synchronisation $(\overline{\kappa(\tau)} = 0.63 \pm 0.00)$ occurs for $g_{ton} = 8\,nS$ and $\tau_i = 14\,ms$ at $8\,s \leq t \leq 10\,s$. The network was stimulated with a constant current $I_{stim} = 0.4\,nA$.

d

e

Figure 9: (cont.) **Enhanced network synchronisation emerges as tonic inhibition is strengthened and synaptic time constants are prolonged.** g_{ton} and τ_i are increased every $2\,s$ in steps of $2\,nS$ and $1\,ms$ respectively. **d** $g_{ton} = 12\,nS$ and $\tau_i = 16\,ms$ at $t = 12\,s$ mark the end of the synchronisation rebound with $\kappa(\tau)$ decreasing 0.42 ± 0.00 and population frequency decelerating to $\overline{f} = 18.04 \pm 0.04\,Hz$. **e** Further increases in propofol dosage cause a gradual weakening of global network activity ($g_{ton} geq 14\,nS$, $\tau_i \geq 17\,ms$, and $t \geq 14\,s$), whose frequency eventually decays to $\overline{f} = 2.74 \pm 0.02\,Hz$ with a synchronisation of $\kappa(\tau) = 0.08 \pm 0.00$ at $t = 22\,s$. The network was stimulated with a constant current $I_{stim} = 0.4\,nA$.
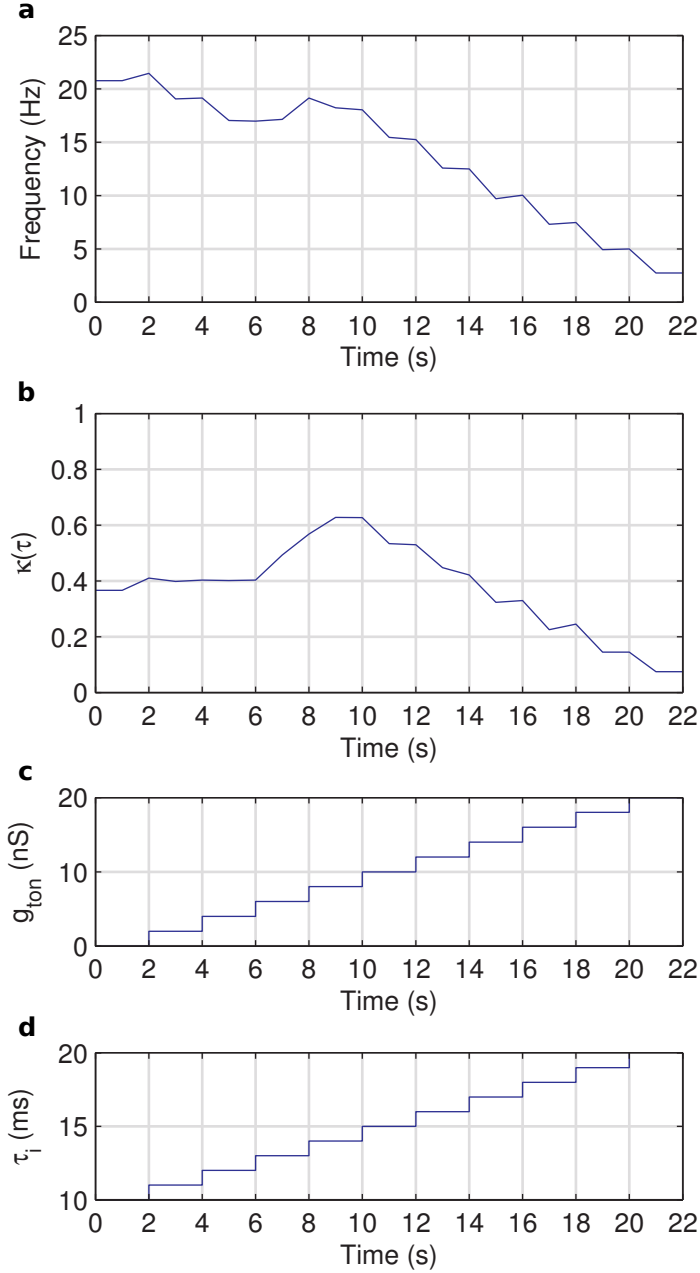
Figure 10: **Enhanced network synchronisation emerges as tonic inhibition is strengthened and synaptic time constants are prolonged. a** The network synchronisation follows a bump-like pattern, increasing from a baseline of $\overline{\kappa(\tau)} = 0.41 \pm 0.01$ between $0\,s \leq t \leq 6\,s$ to a maximum of $\overline{\kappa(\tau)} = 0.63 \pm 0.00$ for $g_{ton} = 8\,nS$ and $\tau_i = 14\,ms$ at $8\,s \leq t \leq 10\,s$. Further anaesthetic dosages gradually lower the network synchronisation. **b** The network frequency follows a bump-like pattern, decelerating between $0\,s \leq t \leq 6\,s$ and then accelerating to a maximum of $\overline{f} = 19.13 \pm 0.17\,Hz$ for $g_{ton} = 6\,nS$ and $\tau_i = 13\,ms$ at $6\,s \leq t \leq 8\,s$. Further anaesthetic dosages gradually decelerate the network frequency. **c** g_{ton} is increased from an initial value of $0\,nS$ in steps of $2\,nS$ every $2\,s$. **d** τ_i is increased from an initial value of $10\,ms$ in steps of $1\,ms$ every $2\,s$.